Adaptive and maladaptive consequences of deregulation in a bacterial gene regulatory network

Rhea Vinchhi*, Chetna Yelpure*, Manasvi Balachandran and Nishad Matange#

Department of Biology, Indian Institute of Science Education and Research, Dr. Homi Bhabha Road, Pashan, Pune 411008

*Equal Contribution

Correspondence nishad@iiserpune.ac.in

Abstract

The archetypal PhoQP two-component system from Enterobacteria regulates crucial pathways like magnesium homeostasis in *Escherichia coli* and virulence factor expression in *Salmonella enterica*. Previously we had reported that a laboratory strain of *E. coli* rapidly accumulated loss-of-function mutations in the *mgrB* gene, a negative feedback regulator of PhoQP, when evolved in the presence of the antibiotic trimethoprim (Patel and Matange, eLife 2021) [1]. Hyperactive PhoQP enhanced the expression of dihydrofolate reductase, target of trimethoprim, resulting in antibiotic tolerance. Here we ask, firstly, how important are mutations in *mgrB* for the evolution of trimethoprim resistance? We report that MgrB-loss, though itself only mildly beneficial, facilitates the evolution of resistance by enhancing the fixation probability of trimethoprim-resistant bacteria under selection. Secondly, we investigate why negative feedback may be needed in the PhoQP system. We show that under drug-free conditions MgrB is required to mitigate the fitness costs of pervasive gene dysregulation by hyperactive PhoQP. Using RNA-seq transcriptomics and genetic analyses, we demonstrate that PhoQP-hyperactivation perturbs the balance of RpoS and RpoD-regulated transcriptional programs, and spontaneous mutations in *rpoS* rectify this imbalance. We propose that relative adaptive and maladaptive consequences of deregulation explain the evolution of negative feedback in bacterial gene regulatory networks.

Introduction

Signal transduction pathways perform the vital function of altering cellular physiology in response to the environment. Signaling cascades often culminate in gene expression states that dictate the behavior of cells and facilitate adaptation to stressful environments. Biochemical and genetic experiments have elucidated the roles of individual signaling cascades in detecting stimuli at the cell surface, transducing this signal intracellularly and modulating gene expression by changing activation states of transcription factor/s. Building on this information, systems-level approaches have revealed that signaling proteins are organized into networks, often referred to as gene regulatory networks [2, 3]. Organization of regulatory proteins into networks not only brings in robustness and exquisite control, but also allows for crosstalk between signaling cascades, ultimately shaping which genes are expressed and to what extent [2-4].

A ubiquitous feature of gene regulatory networks, seen from bacteria to humans, is the presence of feedback [2, 3, 5-8]. Positive feedback in regulatory networks ensures rapid 'switch-like' behavior in response to an activating signal [8, 9]. It allows for bistability, i.e., the existence of two relatively stable transcriptional states [10]. In Gram positive bacteria such as *Bacillus subtilis*, bistability plays an important role in governing cell cycle and developmental programs like sporulation [10]. Negative feedback on the other hand dampens, restricts, or resets activation levels of a signaling network. Negative feedback is thought to be corrective and is required to calibrate levels of gene expression and buffer noise [4, 11, 12]. Corrective feedback has been shown to facilitate adaptation in bacterial signaling as well as linearize gene expression responses [13].

The major signaling proteins used by bacteria are two-component systems [14-16]. The first component, referred to as 'sensor kinase', auto-phosphorylates at a conserved histidine residue upon activation. It then transfers its phosphate group to a conserved aspartate residue on a second protein, called the 'response regulator', which is usually a transcription factor itself. Phosphorylation status of the response regulator directly alters its ability to bind to gene promoters and modify gene expression [14, 16]. Several variations on this basic schema are observed in nature, including dual kinase-phosphatase activity of the sensor kinase [17], multiple phosphorelay steps [14, 18] and crosstalk between non-cognate kinases and response regulators [19, 20]. Two-component systems across bacteria orchestrate responses to a wide range of cues such as metal ions [21], pH [22], nutrients [23], antimicrobial peptides [24], quorum sensing molecules [25] and cell envelope stress [26, 27]. More recently, two-component sensor kinases have been proposed as novel targets for the design of antimicrobials owing to their association with drug resistance in several clinically relevant bacterial species [28-30].

Two-component signaling pathways are important substrates for adaptive evolution in bacteria and mutations in two-component signaling proteins are responsible for adaptation to adverse environments. For instance, sequence variation in the EvgAS two-component system is implicated in modulating the survival of *Escherichia coli* strains in low pH [31]. Similarly, mutations in the DosR-DosS-DosT system in the Beijing lineage of *Mycobacterium tuberculosis* have been associated with hypervirulence [32, 33]. We showed previously that loss-of-function mutations in the *mgrB* gene are rapidly enriched in *E. coli* bacteria that were exposed to the antibiotic trimethoprim [1]. The *mgrB* gene codes for a small membrane protein that inhibits the PhoQP two-component system by binding to the sensor kinase PhoQ [34, 35]. Expression of *mgrB* is itself activated by PhoP, setting up a negative feedback loop

[34, 36, 37]. Loss of functional MgrB resulted in PhoQP-dependent overproduction of dihydrofolate reductase (DHFR) [1, 38], which conferred tolerance to trimethoprim [1]. Interestingly, loss of functional *mgrB* in clinical strains of *Klebsiella pneumoniae* [39] and *Enterobacter cloacae* [40] is causally linked to resistance to colistin , a last-resort antibiotic, demonstrating that deregulation of PhoQP can be beneficial in different bacterial species under antibiotic pressure. In this study, we build on our earlier observations to investigate how crucial mutational loss of negative feedback in PhoQP is for the evolution of trimethoprim resistance in *E. coli*, and why negative feedback may have evolved and is maintained by two-component signaling pathways.

Results

Mutations in *mgrB*, *folA* and *rpoS* genes drive adaptation to trimethoprim in laboratory-evolved *E. coli*

In our laboratory evolution experiments loss of functional *mgrB* was the first mutational event in *E. coli* adapting to trimethoprim [1]. Long term antibiotic exposure led to adaptive sweeps involving mutations in 2 other genes i.e., *folA*, which codes for dihydrofolate reductase (DHFR) and *rpoS*, which codes for the enterobacterial stationary phase sigma factor [1]. While mutations in *mgrB* and *folA* directly enhanced trimethoprim resistance, *rpoS*-mutations enhanced fitness without altering drug IC_{50} [1]. To test whether these 3 loci reproducibly accumulated mutations during the evolution of trimethoprim resistance, we sequenced the genomes of 3 randomly picked resistant isolates from 3 independent lineages of *E. coli* after 350 generations of evolution in trimethoprim. Mutations in *folA* were found in isolates from 2 of the 3 lineages, while *mgrB* harboured mutations in all 3 lineages (Figure 1, Supplementary File 1). Like *mgrB*, *rpoS* mutations too were found across all 3 lineages (Figure 1, Supplementary File 1). Though mutations in several other genes were also found (Supplementary File 1), *folA*, *mgrB* and *rpoS* were the only loci that harboured mutations consistently across lineages, reinforcing their role as the primary hotspots for adaption to trimethoprim.

Mutational loss of *mgrB* facilitates evolution of trimethoprim resistance

By itself, loss of *mgrB* led to a mild enhancement in drug IC_{50} [1]. Despite this, *mgrB* was consistently mutated across independently evolved trimethoprim-resistant bacteria (Figure 1). This observation suggested that though *mgrB*-deficiency alone had only a small effect on drug resistance, it may serve a facilitatory role during adaptation to trimethoprim. To empirically test this idea, we asked, firstly, whether it was possible for *E. coli* to evolve resistance without implicating *mgrB* and secondly, if resistance did evolve without mutations in *mgrB*, how it would impact the rate of resistance evolution.

In strain competition experiments, *E. coli ΔmgrB* showed a dose-dependent increase in relative fitness in trimethoprim-supplemented media (Figure 2A). High concentration of Mg^{2+} (5-10 mM) in growth media, which is known to inhibit PhoQ activity [22, 41] completely neutralized this fitness advantage of *mgrB*-deficiency (Figure 2A). Thus, loss of MgrB was only advantageous for *E. coli* under conditions in which PhoQP was active. Based on this result, we established 6 evolving lineages (1, 2, 3: High Mg^{2+}; 4, 5, 6: Low Mg^{2+}) that were exposed to sub-MIC trimethoprim (100 ng/mL) under conditions of high or low PhoQP activity for ~210 generations (Figure 2B). We argued that, since PhoQP would be active only in low Mg^{2+}, these lineages alone would evolve mutations in *mgrB*, allowing us to dissect out its role in the evolution of resistance. In all three Low Mg^{2+} lineages, trimethoprim-resistant bacteria were rapidly fixed (i.e. frequency >0.9) within the first 50 generations of evolution (Figure 2C). In contrast, High Mg^{2+} lineages evolved resistance at much slower rates, and resistant bacteria were unable to reach fixation over the duration of the experiment (Figure 2C). To ensure that this effect was due to the activity of PhoQP and not an independent effect of Mg^{2+}, we established 3 independent evolving lineages starting with an isogenic *E. coli ΔphoP* strain in low Mg^{2+} media supplemented with trimethoprim (Figure 2B). In these populations too, trimethoprim-resistant bacteria did not get fixed and remained at low frequencies even after 200 generations of evolution (Figure 2C). Thus, low/no active PhoQP severely impeded the establishment of trimethoprim-resistance in *E. coli* populations.

Genome re-sequencing of 3 randomly picked resistant isolates from each of the lineages confirmed that, as expected, mutations in *mgrB* occurred in all Low Mg^{2+} isolates (Figure 2D, Supplementary File 2). In contrast, none of the isolates from High Mg^{2+} and *ΔphoP* lineages harboured *mgrB*-mutations (Figure 2D, Supplementary File 2). Importantly, all 27 sequenced trimethoprim-resistant isolates harboured mutations at the *folA* locus, either in the gene promoter or in the coding sequence (Figure 2D, Supplementary File 2). Genome sequencing of the entire population further confirmed these findings (Supplementary File 2). These results demonstrated that mutations in *folA* were sufficient for the evolution of trimethoprim-resistance. However, *mgrB*-mutations, though not necessary for the evolution of resistance, facilitated fixation of resistant bacteria under trimethoprim selection.

Epistasis between *mgrB* and *folA* facilitates the fixation of trimethoprim resistant bacteria

We next investigated the mechanism underlying the facilitatory role played by *mgrB*-loss. Intergenic epistasis is a well-known determinant of the mutational landscape of resistant bacteria evolving at sub-MIC drug [42]. Therefore, we first assessed whether mutations in *mgrB* were epistatic with drug-resistant *folA* alleles. For these analyses we chose representative strains that harboured mutations in *mgrB* alone, *folA* alone (coding region and its promoter) or at both loci and calculated fold-IC_{50} values over wild type. Loss of *mgrB* alone (*E. coli ΔmgrB*) resulted in a marginal enhancement in IC_{50} of ~3-fold over wild type (Figure 3A). On the other hand, isolates harbouring either a missense mutation in the *folA* gene (Isolate Tmp^R-*folA*-Trp_{30}Arg) or a promoter-up mutation (Isolate Tmp^R-*folA*-C_{-35}T) had significantly higher values of fold-IC_{50} (Figure 3A). Based on a non-epistatic/additive model [42], we expected ~152-fold or ~41-fold increase in IC_{50} of strains harbouring *mgrB*-mutations in addition to the *folA*-C_{-35}T and *folA*-Trp_{30}Arg alleles respectively (Figure 3A). Deviation from these expected values would indicate epistasis between *mgrB* and *folA*. We selected resistant isolates Tmp^R-A and Tmp^R-B, derived from our long-term evolution lines to test this prediction. Tmp^R-A harboured mutant *mgrB* and *folA*-C_{-35}T, while Tmp^R-B harboured mutant *mgrB* and *folA*-Trp_{30}Arg. Interestingly, IC_{50} values of both isolates deviated from expectation, but in opposite ways. Though both strains had higher IC_{50} values than *mgrB*/*folA* mutants alone, Tmp^R-A showed "less-than-additive" effect or magnitude epistasis, while Tmp^R-B showed "greater-than-additive" or synergistic epistasis (Figure 3A). To verify that the observed effects could be attributed to hyperactive PhoQP we deleted the *phoP* gene from Tmp^R-A and Tmp^R-B. Indeed, deleting *phoP* from Tmp^R-A led to only a ~10 % reduction in fold-IC_{50} while Tmp^R-B showed close to ~80 % reduction in fold-IC_{50} (Figure 3A), corroborating our results. These experiments showed that mutations in *mgrB* enhanced the IC_{50} values of bacteria harbouring *folA* mutations, but this effect was more pronounced for coding mutations than promoter mutations.

In parallel, we also analysed the expression level of *folA* in these resistant strains. Loss of functional MgrB alone led to ~2 fold higher levels of *folA* transcript than wild type (Figure 3B). Likewise, Isolate Tmp^R-B also showed ~2 fold higher *folA* transcript, while Tmp^R-*folA*-Trp_{30}Arg had comparable *folA* expression as wild type (Figure 3B). On the other hand, the Tmp^R-*folA*-C_{-35}T showed massive overproduction of *folA*, which was not detectably higher in strain Tmp^R-A (Figure 3B). Thus, *mgrB*-mutations enhanced the expression of wild type or missense alleles of *folA*. However, the effect of *mgrB*-mutation was marginal if cis-regulatory changes in the *folA* promoter were present as the latter masked the effects of hyperactive PhoP. The strongly correlated trends between IC_{50} values and *folA* expression demonstrated

198 that the molecular mechanism behind the observed epistasis was MgrB's influence on *folA*
199 expression levels.
200
201 Could this genetic interaction explain why mutations in *mgrB* facilitated fixation of resistant
202 bacteria? To answer this question, we calculated the frequency at which resistant strains
203 harboring different mutation combinations could establish over a large excess of a drug-
204 sensitive competitor in the presence and absence of sub-MIC trimethoprim (100 ng/mL)
205 (Figure 3C). Competitions (144 replicates for each strain combination) were set up with wild
206 type *E. coli* at a starting ratio of $1:10^7$ in favour of wild type to mimic initial stages of
207 evolution when a resistant mutant first emerges in an ancestrally sensitive population (Figure
208 3C). After 24 hours of competition, 0.5 % of the mixed culture was passaged into LB media
209 containing trimethoprim at the MIC of wild type (1 μg/mL). Growth at this concentration of
210 trimethoprim would indicate that the resistant mutant had been enriched >10-fold during the
211 competition (Figure 3C). Wild type bacteria alone and competitions in the absence of
212 trimethoprim were used as controls. Indeed, strains Tmp^R-A and B had higher frequencies of
213 establishment than Tmp^R-*folA*-$C_{-35}T$ and Tmp^R-*folA*-$Trp_{30}Arg$ demonstrating the impact of
214 *mgrB* mutations as facilitators of resistance evolution (Figure 3D). Further, *mgrB*-mutation
215 enhanced the frequency of establishment of the *folA*-$Trp_{30}Arg$ allele to a greater extent than
216 *folA*-$C_{-35}T$, in line with the differential epistatic effects between these mutations (Figure 3D).
217 Thus, we concluded that *mgrB*-mutations facilitated the fixation of bacteria with mutations in
218 *folA* under drug pressure, which could be explained mechanistically by epistasis between
219 *mgrB* and *folA* loci.
220
221 **MgrB is retained by *E. coli* to prevent costs of PhoQP hyperactivation**
222
223 Since loss of functional *mgrB* was frequent and beneficial under antibiotic pressure, we
224 wondered why negative feedback may be needed in the PhoQP system in the first place. To
225 address this question, we first assessed the evolutionary conservation of *mgrB* across PhoQP-
226 expressing bacteria. The PhoQP system is restricted to the Order Enterobacterales [43].
227 Within this order, the *phoQ* gene was found in all bacterial families except Budviciaceae,
228 indicating that PhoQP may have emerged after the divergence of Budviciaceae from the other
229 6 families (Figure 4A). The *mgrB* gene was present in representative members of 4 of the 6
230 families that harboured *phoQ*, namely Morganellaceae, Yersiniaceae, Pectobacteriaceae and
231 Enterobacteriaceae, but not in Erwiniaceae and Hafniaceae (Figure 4A). Phylogenetic
232 relationships between these families [44] suggested that Erwiniaceae and Hafniacieae may
233 have independently lost *mgrB* during evolution. We next examined the distribution of *phoQ*
234 and *mgrB* among members of family Enterobacteriaceae, to which *E. coli* belongs (Figure
235 4B). Among 61 query species examined by us, we found that most harboured both, *phoQ* and
236 *mgrB*. A few exceptions were also identified, such as Izhakiella, Rosenbergiella,
237 Limnobaculum and some species of Candidatus, which code for PhoQ but not MgrB (Figure
238 4B). Once again, their phylogenetic relationships suggested that these genera represented
239 independent gene-loss events (Figure 4B). Taken together, these analyses showed that
240 multiple independent events of loss of the *mgrB* gene have occurred during bacterial
241 evolution. However, most extant bacterial species preserved a functional *mgrB* gene,
242 indicating that negative feedback in PhoQP is dispensable but desirable.
243
244 In line with this idea, there was no detectable difference in the growth characteristics of wild
245 type *E. coli* and its isogenic *mgrB* knock-out strain under standard laboratory conditions
246 (Figure 5A). However, when *E. coli ΔmgrB* was directly competed against *ΔlacZ*-marked
247 wild type, a significant fitness cost ($w_{\Delta mgrB} = 0.83 \pm 0.03$) was observed (Figure 5B, C). The

248 fitness cost of *mgrB*-deficiency was due to hyperactivation of PhoQP since addition of high
249 Mg^{2+} to growth media or deletion of *phoP/Q* genes restored relative fitness to wild type
250 levels (Figure 5B, C). Our earlier work has shown that loss-of-function mutations in *rpoS* that
251 occurred spontaneously during long term evolution in trimethoprim improved the fitness of
252 *mgrB*-deficient *E. coli* in the drug-supplemented media without enhancing IC_{50} [1]. Since
253 RpoS is itself an indirect target of PhoQP signaling and known to be overproduced in *mgrB*-
254 knock out bacteria [45], we asked whether loss of *rpoS* could compensate for the fitness costs
255 of *mgrB*-deficiency in drug-free media as well. This was indeed the case and deletion of *rpoS*
256 restored the relative fitness of an *mgrB*-knockout strain (Figure 5B, D). Like *rpoS*, deletion of
257 *iraM*, which links *rpoS* to PhoQP signaling [45], also rescued the fitness cost of *mgrB*-
258 deficiency (Figure 5B, D). Thus, we concluded that the costs of *mgrB*-deficiency could be
259 mechanistically traced to hyperactivation of PhoQP and over-production of RpoS, explaining
260 why negative feedback may be needed in the PhoQP system.
261
262 **Pervasive gene dysregulation in *mgrB*-deficient *E. coli* is rectified by mutations in *rpoS***
263
264 We next sought to understand the molecular mechanistic basis for the cost of *mgrB*-
265 deficiency and the compensatory role of *rpoS*-mutations. To do this, we compared the whole
266 transcriptomes of trimethoprim-resistant isolates from early and late time points of our long-
267 term evolution lines using RNA-seq. The isolates Tmp^R-A and Tmp^R-B were chosen from
268 early time points since they both harboured loss-of-function mutations at the *mgrB* locus and
269 had wild type *rpoS* (Figure 6A). Since both isolates also harboured other mutations,
270 comparing the transcriptomes of Tmp^R-A and Tmp^R-B would help to identify *mgrB*-specific
271 gene regulatory effects. The isolate Tmp^R-C was chosen from a later time point as it
272 harboured the same mutation in *mgrB* as Tmp^R-B and an inactivating mutation in *rpoS*
273 (Figure 6A). All three isolates also harboured mutations in the *folA* gene (Tmp^R-B, C) or its
274 promoter (Tmp^R-A) (Figure 6A).
275
276 At the global level, the differential gene expression profiles of Tmp^R-A and Tmp^R-B were
277 very similar and strongly correlated (linear correlation coefficient $R^2 = 0.59$) (Figure 6B). On
278 the other hand, Tmp^R-B and Tmp^R-C showed significant differences in their transcriptomes
279 (linear correlation coefficient $R^2 = 0.19$) (Figure 6C). Next, we turned our attention
280 specifically to genes of the PhoP-regulon. A total of 58 genes are known direct targets of the
281 PhoQP system in *E. coli* [46-48]. We noted that despite the presence of *mgrB*-mutations,
282 majority of the PhoP-regulon remained unaltered in all 3 isolates (Figure 6D, Supplementary
283 File 3). For instance, the levels of PhoP-targets such as the *acrAB* efflux pump and the *glg*
284 glycogen metabolism operon were unaffected by the loss of *mgrB*. These genes are regulated
285 by other transcription factors in addition to PhoP, including master regulators such as CRP
286 [46-48], and hence may be less sensitive to the activation status of PhoP. Hyperactivation of
287 PhoQP was reflected most dramatically in the overexpression of genes that are solely
288 regulated by PhoP, such as the *phoQP* operon itself or the magnesium transporter *mgtA*
289 (Figure 6D, F, Supplementary File 3).
290
291 A subset of PhoP-targets is also regulated by the RpoS sigma factor [46-48]. Targets of PhoP
292 and RpoS include genes that form the 'acid-resistance regulon' such as the '*gad*' and '*hde*'
293 operons [45]. In Tmp^R-A and B most of the PhoP-RpoS co-regulon showed mild to high
294 over-expression compared to wild type (Figure 6E, Supplementary File 3). However, in
295 Tmp^R-C, several of these genes were significantly down-regulated relative to wild type,
296 indicating that mutation in *rpoS* overrides the effects of PhoQP hyperactivation and
297 compensates for the hyperactivity of PhoP (Figure 6E, Supplementary File 3). We confirmed

these findings using qPCR for representative genes and found the results to be in line with the RNA-seq transcriptomics data (Figure 6F).

Curiously, we noticed that there were several differentially expressed genes between isolates that are not direct targets of PhoP or RpoS (Supplementary File 3). Particularly striking among them were genes that were significantly down-regulated in Tmp^R-A and Tmp^R-B but restored to wild type levels in Tmp^R-C (Figure 6C, Supplementary File 3). A closer look at this sub-set of genes revealed that a majority of them were transcribed in an RpoD-dependent (i.e. Sigma 70-dependent) manner and were involved in growth and metabolism such as *lpxT* (lipid A metabolism), *ccmA-D* (cytochrome maturation) and *rcnA-B* (metal ion homeostasis) (Figure 6C, G, Supplementary File 3). Similarly, several RpoD-regulated tRNA genes were also expressed to a higher level in Tmp^R-C, compared to Tmp^R-A and Tmp^R-B (Figure 6G, Supplementary File 3). It is well-established that RpoS and RpoD compete for the same binding site on RNA polymerase and competition between these two sigma factors dictates whether *E. coli* expresses genes required for growth and division (RpoD-regulated) or stress-response and stationary phase (RpoS-regulated) [49]. The dysregulation of RpoD-target genes in Tmp^R-A and B thus suggested that precocious RpoS activation due to *mgrB*-deficiency tilted the balance in favour of the RpoS-transcriptional program, which was compensated at later stages in evolution by mutations in *rpoS*. Based on these results, we concluded that loss of *mgrB* led to pervasive perturbation of gene expression beyond the PhoP-regulon, its primary target, to secondary and tertiary effects on the expression of RpoS- and RpoD-regulated genes respectively. Mutations in *rpoS* restored several of these secondary and tertiary gene regulatory effects.

RpoS-RpoD imbalance explains the fitness costs of MgrB-deficiency in *E. coli* and justifies the need for negative feedback in the PhoQP system

Based on the above result, we hypothesized that the cost of *mgrB*-loss may arise either due to overproduction of RpoS-regulated genes or the repression of RpoD-regulated genes. To test which of these two possibilities was true, we first generated knockouts of the *hdeD*, *gadW* and *gadE* genes (co-targets of RpoS and PhoP) in an *mgrB*-deficient background and asked whether these gene deletions could rescue the fitness cost of the *mgrB* knockout. These specific genes were selected since they are master regulators of the acid-resistance regulon and were up-regulated in Tmp^R-A and B, but significantly repressed in Tmp^R-C. However, the fitness of the *mgrB* knockout was unaffected by deletion of these genes (Figure 7A) ruling them out as the source of the observed fitness cost. Next, to test whether the imbalance between RpoS and RpoD could explain the costs of *mgrB*-deficiency, we deleted the *rsd* or *crl* genes from the *mgrB*-knockout and measured relative fitness. Rsd is an inhibitor of RpoD [50, 51], while Crl is potentiator of RpoS [52], and loss of either protein would tilt the balance in favour of RpoD-regulated transcription. Indeed, deletion of *rsd* or *crl* rescued the costs of the *mgrB*-knockout strain (Figure 7A). Finally, we traced how the competitive ability of *E. coli ΔmgrB* changed with growth phase. We found that in the logarithmic phase, when RpoD is known to be higher, there was no detectable difference between *mgrB*-deficient and wild type bacteria in a mixed culture. However, the competitive disadvantage of *E. coli ΔmgrB* became evident at the onset of stationary phase when the shift from RpoD to RpoS-mediated transcription is known to occur (Figure 7B). This effect too was compensated by deletion of *rpoS* (Figure 7B). These results confirmed that pervasive transcriptional dysregulation of gene expression due to hyperactive PhoQP explained the costs of *mgrB* deficiency and provided a mechanistic explanation for why negative feedback is retained by this two-component system during evolution.

Discussion

Loss of functional MgrB occurs spontaneously under antibiotic pressure and is associated with resistance to trimethoprim in *E. coli* [1, 38] and colistin in *K. pneumoniae* [39]. Being a negative feedback regulator of the PhoQP two-component system, absence of MgrB hyperactivates PhoP and leads to overexpression of several of its targets [37, 45]. In this study, we have used the PhoQP/MgrB two-component system from *E. coli* to ask what the contribution of gene regulatory evolution is to antimicrobial resistance in bacteria. Our results demonstrate that loss of checks and balances such as negative feedback in gene regulatory pathways can be adaptive for bacteria under antibiotic pressure. Further, deregulating gene expression has the potential to amplify the phenotypes of other resistance-conferring mutations and hence facilitate the evolution of high level antibiotic resistance. Importantly, we have also shown that deregulation of signalling pathways has pervasive effects on the wider gene regulatory network of cells, which are maladaptive. As a result, it is accompanied by a fitness cost that must be compensated through additional evolutionary adaptation (Figure 8).

Increased expression of drug-targets, most commonly due to mutations in gene promoters or transcription factors, is reported in many antibiotic-resistant bacterial pathogens. For instance, mutations in the promoter of the *pbp4* gene in beta-lactam resistant *Staphylococcus aureus* [53], missense mutations in *mgrB* or *phoQ* in colistin-resistant *Klebsiella pneumoniae* [54] and *inhA* promoter mutations in isoniazid-resistant *Mycobacterium tuberculosis* [55] are all frequently-encountered, clinically-relevant mechanisms of antibiotic resistance. The main role of regulatory mutations is assumed to be to enhance bacterial fitness by increasing expression of the drug target. In our study, loss of functional MgrB, and associated overexpression of *folA* did indeed confer a fitness advantage to *E. coli* challenged with trimethoprim. By itself, this benefit was incremental and would normally be considered clinically irrelevant. However, *mgrB*-loss contributed significantly to the evolution of high-level trimethoprim resistance by synergistic epistasis with missense mutations in *folA*. Consequently, *mgrB*-mutations were the most frequent genetic change in laboratory-evolved trimethoprim resistant bacteria despite the small stand-alone impact on drug IC_{50}/MIC. Thus, our study throws light on another, perhaps more significant role of regulatory mutations as facilitators of antimicrobial resistance evolution through epistasis. Phenomenologically similar ideas have been proposed by a few other studies, though in these cases the mechanistic bases were unclear. For instance, antibiotic-induced alterations in global gene expression promoted the fixation of resistance-conferring mutations in *E. coli* challenged with amoxicillin and tetracycline [62]. Similarly, expression-modifying mechanisms have been shown to serve as "latent defences" that bacteria can exploit in order to adapt to antibiotics [63]. Taken together, the role played by regulatory mutations in facilitating the evolution of antimicrobial resistance is likely to be more wide-spread than understood so far and requires greater attention.

Based on our previous work, as well as work from other groups, we explain the mechanism of epistasis between *mgrB* and *folA* as follows. Missense mutations in DHFR can structurally destabilise the protein and reduce its steady state levels [56, 57]. Hyperactive PhoP is likely to compensate for this effect by increasing the transcription of mutant DHFR in the bacterial cell, resulting in high levels of drug resistance. Interestingly, we have shown earlier that loss of Lon protease activity also shows synergy with unstable drug-resistant DHFR mutants by increasing their *in vivo* half-life [61]. Thus, increasing expression level of mutant DHFRs,

regardless of mechanism, can facilitate high-level resistance evolution. This mechanism is consistent with our observation that coding mutations in DHFR synergize with *mgrB*-mutations, while mutations in the *folA* promoter don't do so. It is important to note here that the number of possible resistance-conferring coding-region mutations in *folA* is much higher than promoter mutations [1, 58-60]. Thus, by-and-large *mgrB* is more likely to synergistically enhance the resistance level of *folA*-mutant bacteria than not.

We propose that characterising gene regulatory evolution in drug-resistant bacteria may help to identify new points of intervention for AMR pathogens. Our study shows that "switching-off" PhoQP signalling sensitized resistant *E. coli* to trimethoprim as well as retarded resistance evolution. Sensitization strategies such as this one are potential solutions to the current AMR crisis. A few approaches to achieve sensitization to antibiotics that have been explored so far have used adjuvant molecules that enhance the concentration of antibiotics in bacterial cells [64]. For instance, efflux pump inhibitors like verapamil have been explored as a possible mode of re-sensitising multi-drug resistant bacteria [65]. Similarly, cell wall perturbing polymers can also potentiate the activity of some antibiotics by enhancing their penetration into bacterial cells [65, 66]. Our work shows that modifiers of two-component system-regulated gene expression may serve as an additional or alternative sensitization strategy. Though our results have been limited to trimethoprim resistant *E. coli,* several two-component systems are associated with resistance to antibiotics in different bacteria, often due to direct activation by the antibiotic [28]. Thus, this strategy for sensitization is likely to have wide application. Indeed, there are also potential advantages to targeting two-component sensor kinases for therapeutic purposes. Since they are not found in human cells, pharmacologically inhibiting two-component may produce fewer off-target effects in the host. Further, being cell envelope proteins with known ligands, inhibitor design may be facilitated. Finally, modulation of bacterial gene expression has not yet been targeted therapeutically and hence is unlikely to be confounded by pre-existing resistant mutants in clinical strains. These interventions may also serve the purpose of "evolution-proofing" of new antibiotics since they are likely to slow down the evolution of resistance as shown by us in this study and could be thought of as prospectively-used adjuvants.

Beyond the evolution of drug-resistance, our study contributes to the understanding of how gene regulatory networks evolve, particularly in the context of the emergence and maintenance of negative feedback. Mathematical modelling coupled with experiments using natural or synthetic genetic circuits have shown that negative feedback can reduce noise in gene regulatory networks [4, 6, 11, 12, 67]. Despite this knowledge, the importance of negative feedback from an evolutionary perspective remains poorly investigated. The only empirically validated basis for the evolution of negative feedback is to enhance mutational tolerance. Marciano et al. used the LexA transcription factor of *E. coli* to demonstrate that negative feedback canalises phenotypes and provides greater tolerance to mutational perturbation [68]. Similar observations were made for the Rox1 protein from *Saccharomyces cerevisiae* where negative feedback stabilised gene expression levels and enhanced mutational robustness [69]. For the PhoQP system, it has been speculated that MgrB may have evolved to optimise the signalling output of PhoQP in environments with varying Mg^{2+} concentrations [34, 36, 37]. Our study provides experimental evidence for an alternative explanation for the evolution of negative feedback in PhoQP, i.e., to prevent pervasive dysregulation of the larger bacterial genetic network. In other words, we propose that negative feedback serves to insulate pathways that can potentially cross-activate, like PhoQP and RpoS transcriptional networks.

We note that wider application of the above idea to other bacteria is contingent on the pervasive gene regulatory effects of PhoQP in different bacterial species. Indeed, the PhoQP regulon has been worked out in a few species other than *E. coli*. We find that in all characterised systems, like in *E. coli*, PhoQP activation leads to gene expression changes that extend beyond the PhoP regulon. For example, in *Pectobacterium versatile* and *Yersinia pestis*, genome-wide transcriptomics and ChIP-seq have revealed that PhoP influences the expression of several genes beyond its direct targets, though the mechanisms aren't yet clear [70-72]. For *E. coli*, our study shows that RpoS overproduction and exclusion of RpoD from RNA polymerase are responsible for activating secondary and tertiary transcriptional programs in response to PhoQP hyperactivity. Interestingly, while Pectobacterium and Yersinia code for RpoS, they lack IraM-like proteins and hence in these species PhoQP may produce pervasive dysregulation of gene expression by other mechanisms [43]. Regardless, a broad gene-regulatory influence of the PhoQP pathway seems to be consistent across bacteria, supporting the idea that a key selection pressure for the maintenance of MgrB may be to limit cross-activation of other transcriptional programs by PhoP. It is important to note here that the requirement for negative feedback is highly contextual, at least in pathways like PhoQP that directly respond to the extracellular medium. Indeed, deregulation of PhoQP by loss of MgrB is itself beneficial in many environments such as acid stress and antibiotics [1, 39, 45, 54]. The multiple instances of loss of *mgrB* across bacterial phylogenies observed by us in the present study may reflect different selection pressures driving evolution of the PhoQP system in different bacteria. Similarly, cross-activation of other regulatory pathways, though costly under the conditions tested by us, may have advantages in more complex environments. For the PhoQP/MgrB system from *K. pneumoniae* this idea has been recently proposed. Bray et al. (2021) [73] demonstrated that loss of MgrB in colistin resistant-*K. pneumoniae* is accompanied by compromised gastrointestinal colonisation efficacy. Like our results, this study too reported the overproduction of RpoS in *mgrB*-deficient *K. pneumoniae*. However, the authors reported that RpoS overproduction was beneficial in a model for pathogen transmission [73]. Thus, life-history and growth context are both likely to have a strong influence on how deregulation of gene expression translates to organismal fitness.

Curiously, the evolution of negative feedback proteins in two-component signalling pathways appears to be the exception rather than the rule. In *E. coli* only 2 systems, i.e. PhoQP and CpxAR have known negative feedback regulator proteins [74]. Our results may throw light on why this is the case. Based on the idea that pervasive gene dysregulation drives the evolution of negative feedback, we propose that the following criteria necessitate the evolution of negative feedback in two-component pathways. Firstly, the system must have a large regulon which increases the chance of its activity translating to changes in organismal fitness across environments. Secondly, the system should have a positive feedback loop, i.e., it should activate its own expression. This is known to be true for the PhoQP system and results in rapid amplification of signalling after activation. Finally, the regulon of the two-component system should be connected to other global regulatory networks, such as RpoS in the case of PhoQP. For *E. coli*, only 3 two-component systems satisfy all these criteria, namely PhoQP, CpxAR and ArcAB, of which 2 have known negative feedback regulators (Figure 9). In the case of ArcAB, we are not aware of negative feedback systems, however we believe that it may be reasonable to look for them in the future. We cannot rule out the role of regulatory RNAs here, several of which are known to be activated by two-component signalling [75]. Further investigation would be needed to test whether their contribution is similar to that of MgrB.

In conclusion, despite extensive mechanistic insights into the functioning of gene regulatory networks, there is relatively less known about how they evolve and are rewired in response to environmental perturbation. Using the PhoQP-MgrB system, we have analysed the immediate and distal effects of deregulation by loss of negative feedback on the cellular transcriptional network. By linking these changes with organismal fitness across relevant environments we have shown how evolution in a gene regulatory network proceeds in response to selection and can drive and modulate evolutionary adaptation.

507 **Materials and Methods**
508
509 **Bacterial strains and culture conditions**
510
511 *E. coli* wild type and its mutants were cultured in Luria-Bertani Broth (LB) or on Luria-
512 Bertani Agar (LA plates). Media were supplemented with trimethoprim and $MgSO_4$ at
513 required concentrations as needed. Kanamycin or chloramphenicol for selection of
514 genetically manipulated strains were added at 30 µg/mL each as needed.
515
516 The strains used in this study are shown in Table 1.
517
518 Table 1. List of strains used in this study.
519

Sr. No.	Strain	Description	Source
1.	*Escherichia coli* K-12 MG1655	Wild type *E. coli*; used as ancestor for evolution experiments and as reference strains for phenotypic and genotypic comparisons	Kind gift from Prof. Sutirth Dey, IISER (Pune)
Gene knockouts generated in E. coli K-12 MG1655			
2.	*E. coli ΔmgrB*	Isogenic knockout of *mgrB* gene (*ΔmgrB::Kan*)	[1]
3.	*E. coli ΔlacZ*	Isogenic knockout of *lacZ* gene (*ΔphoP::Cat*)	[1]
4.	*E. coli ΔphoP*	Isogenic knockout of *phoP* gene (*ΔphoP::Kan*)	[1]
5.	*E. coli ΔphoQ*	Isogenic knockout of *phoQ* gene (*ΔphoQ::Kan*)	[1]
6.	*E. coli ΔiraM*	Isogenic knockout of *iraM* gene (*ΔiraM::Kan*)	[1]
7.	*E. coli ΔrpoS*	Isogenic knockout of *rpoS* gene (*ΔrpoS::Kan*)	[1]
8.	*E. coli Δrsd*	Isogenic knockout of *rsd* gene (*Δrsd::Kan*)	This study
9.	*E. coli Δcrl*	Isogenic knockout of *crl* gene (*Δcrl::Kan*)	This study
10.	*E. coli ΔmgrBΔphoP*	Double knockout of *mgrB* (*ΔmgrB*) and *phoP* (*ΔphoP::Kan*) genes	[1]
11.	*E. coli ΔmgrBΔphoQ*	Double knockout of *mgrB* (*ΔmgrB*) and *phoQ* (*ΔphoQ::Kan*) genes	[1]
12.	*E. coli ΔmgrBΔiraM*	Double knockout of *mgrB* (*ΔmgrB*) and *iraM* (*ΔiraM::Kan*) genes	This study
13.	*E. coli ΔmgrBΔrpoS*	Double knockout of *mgrB* (*ΔmgrB*) and *rpoS* (*ΔrpoS::Kan*) genes	This study
14.	*E. coli ΔmgrBΔrsd*	Double knockout of *mgrB* (*ΔmgrB*) and *rsd* (*Δrsd::Kan*) genes	This study
15.	*E. coli ΔmgrBΔcrl*	Double knockout of *mgrB* (*ΔmgrB*) and *crl* (*Δcrl::Kan*) genes	This study

16.	*E. coli ΔmgrBΔhdeD*	Double knockout of *mgrB (ΔmgrB)* and *hdeD (ΔhdeD::Kan)* genes	This study
17.	*E. coli ΔmgrBΔgadE*	Double knockout of *mgrB (ΔmgrB)* and *gadE (ΔgadE::Kan)* genes	This study
18.	*E. coli ΔmgrBΔgadW*	Double knockout of *mgrB (ΔmgrB)* and *gadW (ΔgadW::Kan)* genes	This study
Strains/Isolates derived from adaptive laboratory evolution and their derivatives			
19.	Tmp^R-*folA*-$C_{-35}T$	Trimethoprim resistant isolate derived from High Mg^{2+} Lineage 1 harbouring the *folA*-$C_{-35}T$ mutation and wild type *mgrB*	This study
20.	Tmp^R-*folA*-$Trp_{30}Arg$	Trimethoprim resistant isolate derived from High Mg^{2+} Lineage 1 harbouring the *folA*-$C_{-35}T$ mutation and wild type *mgrB*	This study
21.	Tmp^R-A	Trimethoprim resistant isolate derived from long term evolution harbouring *folA-$C_{-35}T$* and *mgrB-ΔA_{98}* mutations and wild type *rpoS* (complete genotype in Supplementary File 1)	[1]
22.	Tmp^R-B	Trimethoprim resistant isolate derived from long term evolution harbouring *folA-$Trp_{30}Arg$* and *mgrB::$IS5_{-46}$* mutations and wild type *rpoS* (complete genotype in Supplementary File 1)	[1]
23.	Tmp^R-C	Trimethoprim resistant isolate derived from long term evolution harbouring *folA-$Trp_{30}Arg$*, *mgrB::$IS5_{-46}$* mutations and *rpoS-$Ile_{128}Asn$* mutations (complete genotype in Supplementary File 1)	[1]
24.	Tmp^R-A *ΔphoP*	Derivative of Tmp^R-A harbouring a deletion in the *phoP* gene *(ΔphoP::Kan)*	This study
25.	Tmp^R-B *ΔphoP*	Derivative of Tmp^R-B harbouring a deletion in the *phoP* gene *(ΔphoP::Kan)*	This study

Relative fitness measurements

Relative fitness (w) of various mutant strains of *E. coli* was measured by direct competition with an *E. coli ΔlacZ* strain under appropriate growth conditions. Neutrality of the *ΔlacZ* genetic marker was established by competitions with unmarked wild type *E. coli* under every growth condition tested. The methodology followed is described in Patel and Matange (2021) [1].

Monoculture and mixed culture growth curves

Bacterial strains to be characterised were initially grown overnight to saturation. From saturated cultures, bacteria were passaged (0.1%) into 5 mL LB broth and grown at 37°C, with shaking at 180 rpm. For competitive growth curves, 2.5 µL each of the competing strains were inoculated in 5 mL LB.

Aliquots were taken for measuring bacterial growth periodically until 20-24 hours of growth. Bacterial growth was monitored using optical density (OD) at 600 nm for monocultures and

538 by viable counts (CFU/mL) for mixed culture. For viable counts, aliquots of bacterial cultures
539 were serially diluted and plated on LA supplemented with IPTG (50 µg/mL) and X-Gal (50
540 µg/mL). Plates were incubated for 18-24 hours at 37 ºC and blue and white colonies were
541 counted.
542
543 **Laboratory evolution of trimethoprim resistance**
544
545 The detailed methodology for laboratory evolution of trimethoprim resistance is described in
546 Patel and Matange (2021) [1] and Vinchhi et al. (2023) [76]. Trimethoprim was used at a
547 concentration of 100 ng/mL which corresponds to ~MIC/9. $MgSO_4$ was added to growth
548 media at a concentration of 10 mM wherever appropriate.
549
550 **Genome sequencing of laboratory-evolved trimethoprim resistant isolates**
551
552 Genome sequencing and variant calling for evolved bacteria was carried out as described in
553 Patel and Matange (2021) [1] and Vinchhi et al. (2023) [76]. Sequencing services were
554 provided by Eurofins, India.
555
556 **Genetic manipulations and gene knockout in *E. coli***
557
558 All gene knockouts were generated using P1 transduction by moving kanamycin-resistance
559 marked gene deletions from donor strains taken from the Keio Collection [77, 78] into
560 appropriate recipient strains. Knockouts were confirmed using gene specific PCR on genomic
561 DNA extracted from transductants. Detailed methodology is described in Patel and Matange
562 (2021) [1].
563
564 **Measuring trimethoprim resistance**
565
566 Trimethoprim resistance of *E. coli* strains or trimethoprim-resistant isolates was measured
567 using a broth-dilution assay. IC_{50} values were determined by fitting experimental data to a
568 variable-slope, 4 parameter model using Graphpad Prism (version 9.1.4). Detailed
569 methodology is described in Patel and Matange (2021) [1] and Vinchhi et al. (2023) [76].
570
571 **Establishment propensity of trimethoprim-resistant isolates at sub-MIC drug pressures**
572
573 To estimate the propensity of establishment of trimethoprim-resistant strains, their ability to
574 out-compete a large excess of wild type *E. coli* under sub-MIC trimethoprim selection was
575 evaluated. To set up the primary competitions, trimethoprim-evolved mutant isolate and wild-
576 type *E. coli* were mixed ($1:10^7$), and the mixture was diluted 100 times in a final volume of
577 15 mL LB broth supplemented with 100 ng/mL trimethoprim. This diluted culture was then
578 dispensed into the wells of a sterile 96-well polystyrene plates (200 µL per well), and
579 incubated at 37°C for 24 hours, with shaking at 180 rpm. Next, 1 µL from each well was
580 passaged into 200 µL of LB broth containing 1 µg/mL trimethoprim (i.e. MIC of wild type
581 [1]) in a fresh 96-well plate. This plate was incubated at 37°C for 24 hours with shaking at
582 180 rpm. Only those wells in which mutant bacteria were enriched by >10-fold would show
583 turbidity. The number of wells showing visible growth were noted, and OD_{600} was measured
584 using a plate reader. Two controls were also set up in parallel. For the first control, primary
585 competition was performed in the absence of trimethoprim such that there would be no
586 enrichment of resistant-mutants. The second control had similar number of wild-type cells
587 without the addition of mutant bacteria. This control would indicate the frequency of

588 spontaneous resistant mutants emerging during the competition. OD_{600} values of 144 replicate
589 competitions for each condition were plotted and compared.
590
591 **Sequence and phylogenetic analyses**
592
593 To analyse the distribution of homologs of PhoQ and MgrB from *E. coli* across different
594 bacterial species, the Pfam database [43] was initially mined. Since both proteins were
595 restricted to the Order Enterobacterales further analyses were restricted to this group of
596 bacteria. The phylogenetic relationships of different families under Order Enterobacterales
597 was taken from Adelou et al., 2016 [44]. Type strains from each family were identified using
598 the LPSN (List of Prokaryotic names with Standing in Nomenclature; https://lpsn.dsmz.de/)
599 database [79, 80]. For family Enterobacteriaceae, a maximum likelihood phylogenetic tree
600 was constructed using 61 bacterial species in MEGA-X [81], by using 16s rRNA gene
601 sequences of the type strain of each genus as listed in LPSN [79, 80]. The presence or
602 absence of PhoQ and MgrB in bacterial strains under consideration was determined by three
603 methods: first, directly analysing genome annotation data available on NCBI, second, by
604 performing BLASTn against the genome of the query organism (nucleotide similarity with
605 wild-type *E. coli mgrB*-NCBI Gene ID: 946351 and *phoQ*-NCBI Gene ID: 946326), third, by
606 performing NCBI BLASTp against the proteome of the query organism (amino acid
607 similarity with wild-type *E. coli* MgrB-Uniprot: P64512 and PhoQ-Uniprot: P23837). A
608 positive hit in at least one of the above searches was taken to mean that PhoQ/MgrB were
609 present in the query organism.
610
611 **Gene expression analysis**
612
613 *Transcriptome analyses using RNA-sequencing*
614
615 For RNA-seq, 1% of a saturated culture of wild type and trimethoprim resistant isolates
616 Tmp^R-A, Tmp^R-B and Tmp^R-C was inoculated into 3 mL LB in duplicate and incubated at 37
617 ºC for 3 hours with shaking at 180 rpm. Bacteria were pelleted down using centrifugation and
618 resuspended in 1 mL of RNAlater (Invitrogen) for storage. Subsequent RNA extraction,
619 sequencing and preliminary data analyses were performed by Redcliff Life Sciences (India).
620 Total RNA was extracted using RNAeasy spin columns and quantitated using Qubit and
621 Bioanalyzer. Bacterial rRNA was depleted using Ribozero kit. Bacterial mRNA was then
622 reverse transcribed, library was prepared and quality control was performed using
623 Tapestation platform. Paired end sequencing was performed on Illumina platform with read
624 lengths of 150 bp read length. Processed reads were aligned to the reference genome
625 (NZ_CP025268) using HISTAT2(version 2.1.0). Abundance estimation was done using
626 featureCounts(version1.34.0). Differential gene expression (DGE) analysis was done by
627 comparing the expression of individual genes trimethoprim-resistant strains to wildtype using
628 DESeq2. The output of the DGE analyses were log_2(fold change) values for each gene and P-
629 values to test for statistical significance. Differentially expressed genes were classified into
630 PhoP-regulated, RpoS-regulated and RpoD-regulated based on information available in
631 RegulonDB [47, 48] and Ecocyc [46]. Sigma factors regulating differentially expressed genes
632 were also obtained from RegulonDB [47, 48] and Ecocyc [46].
633
634 *Gene specific quantitative RT-PCR*
635
636 Quantitative RT-PCR was used to validate the findings of RNA-seq. For RNA extraction,
637 appropriate bacterial strains were grown for 3 hours at 37 ºC and pelleted by centrifugation.

638 Total RNA was extracted using TRIzol Reagent (Invitrogen, USA) and quantified
639 spectrophotometrically. RNA quality was evaluated by electrophoresis on a 1% agarose gel
640 and staining with ethidium bromide. Extracted RNA (20µg) was treated with recombinant
641 DNase I (RNAse free) (Takara, Japan) and then cleaned-up using RNeasy spin column
642 (Qiagen, Japan). Prepared RNA was stored at -80 ºC until further use. Reverse transcription
643 reaction was set up using the cleaned-up RNA (~1.6µg) using PrimeScript™ RT reagent Kit
644 (Takara, Japan). The RT reaction was carried out with buffering temperature at 25 ºC for 2
645 mins, cDNA synthesis at 37 ºC for 30 mins. The RT enzyme was inactivated at 85 ºC for 90
646 seconds. Prepared cDNA was serially diluted (10, 100 and 1000-fold) and semi-quantitative
647 PCR were set-up using gene-specific primers (Table 2) to ensure the absence of
648 contaminating genomic DNA contamination and checking for priming efficiency. cDNA was
649 stored at -20 ºC until further use.
650 Quantitative RT-PCR (qPCR) for target genes was performed using TB Green®Premix Ex
651 Taq™ II (Tli RNaseH Plus) (Takara, Japan) and using gene-specific primers listed in Table 2.
652 For each PCR, 20 µL reaction contained 10 µL of 2X TB Green Premix, 0.5 µl each of
653 forward and reverse primers (10 µM stock), 8µl of nuclease-free water and 1 µL of
654 appropriately diluted cDNA. The qPCR reactions were performed on an Eppendorf Realplex2
655 Mastercycler (Eppendorf, Germany) using a two-step protocol with an initial denaturation at
656 95 ºC for 30 seconds, 40 cycles of denaturation at 95 ºC for 5 seconds and annealing and
657 extension for 30 seconds at 60 ºC. A melt curve analysis was performed after 40 cycles of
658 qPCR. 16S rRNA was used as a normalizing internal control to calculate change in
659 expression for all other genes. A known concentration of genomic DNA and its dilutions
660 were used to construct a standard graph for each gene. Fold changes in gene expression for
661 each gene were calculated with respect to the wild type using the standard graph method.
662
663 Table 2. List of primer, cDNA dilution and expected product sizes for qPCR
664

Sr. no.	Gene	Primer sequence (5' to 3')	Amplicon length (bp)	cDNA dilution used for qPCR
1.	16SrRNA (*rrnA*)	Fwd: GCTACAATGGCGCATACAAA	101	1:1000
		Rev: TTCATGGAGTCGAGTTGCAG		
2.	*mgtA*	Fwd: CGGCACAAGCAATGGTGATT	151	1:10
		Rev: GCCATCACCAGCATAAAGCG		
3.	*mgrB*	Fwd: AGTTTCGATGGGTCGTTCTGG	122	undiluted
		Rev: CTGGTTAATGGCACAAATTCCG		
4.	*hdeD*	Fwd: GTGTTGCAGGGGTTATTCGC	142	1:10
		Rev: AGCGTTACAGACACCATCGG		
5.	*gadW*	Fwd: GCTCGGTGATCCTCATTCGT	147	1:10
		Rev: CGATATCCAGTCGTCGCGTA		
6.	*phoP*	Fwd: TCCGAGATCGACAATCGCAA	164	1:10
		Rev: GCGCGTACTGGTTGTTGAAG		
7.	*acrA*	Fwd: TACGCGCTATCTTCCCGAAC	154	undiluted
		Rev: CAACTACCAGTACGGTGGCA		
8.	*folA*	Fwd: GTAACGTGGGTGAAGTCGGT	143	undiluted
		Rev: ACTTCTGCGTCGATATGCGT		

665
666
667
668

Acknowledgements

Funding for this work was provided by the DBT/Wellcome Trust India Alliance Intermediate Fellowship awarded to NM. RV and MB are supported by fellowships from the Indian Institute of Science Education and Research, Pune, India. CY is supported by fellowship from the Department of Biotechnology, Government of India.

Material and Data Availability

All materials such as bacterial strains generated in this study will be shared upon request. Sequencing datasets will be uploaded to Genbank soon (Project:PRJNA741586) and shared on demand if needed.

689 **Figures**

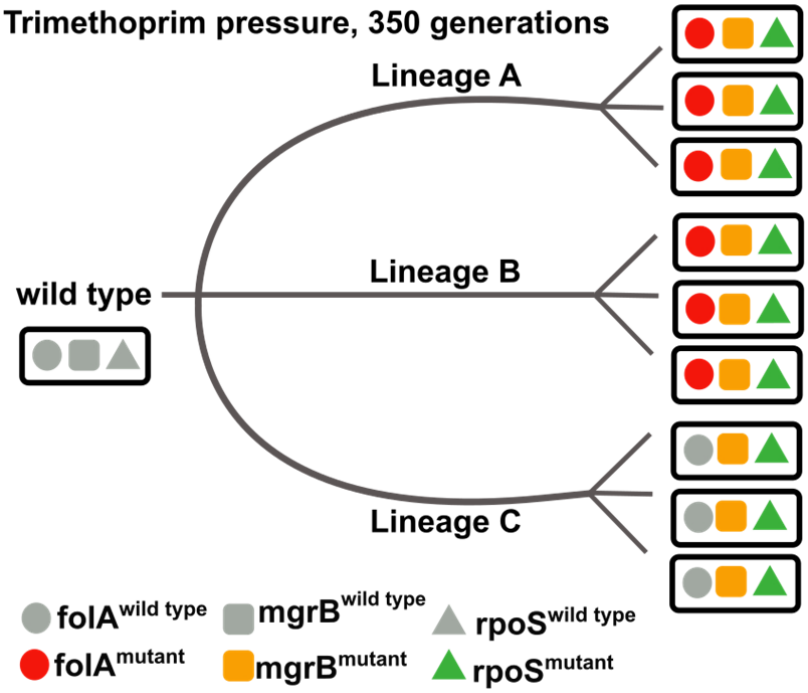

690
691
692 **Figure 1. Genetic changes associated with trimethoprim-resistance evolution.**
693 Diagrammatic representation of three gene loci, *folA* (circle), *mgrB* (square) and *rpoS*
694 (triangle) across 3 randomly selected trimethoprim-resistant isolates from 3 independently
695 evolved lineages (A, B and C) [1]. Each lineage was subjected to sub-MIC trimethoprim (300
696 ng/mL) for ~350 generations after which resistant bacteria were isolated on media
697 supplemented with 1 µg/mL of trimethoprim (i.e. MIC of wild type). Wild type *folA*, *mgrB*
698 and *rpoS* are represented in gray, while coloured symbols are used to represent mutant loci.
699 All mutations in *mgrB* and *rpoS* are known/predicted to be loss of function mutations.
700 Mutations in *folA* were in the coding region or the gene promoter. A complete list of
701 mutations detected in each of the isolates is given in Supplementary File 1.
702

703
704

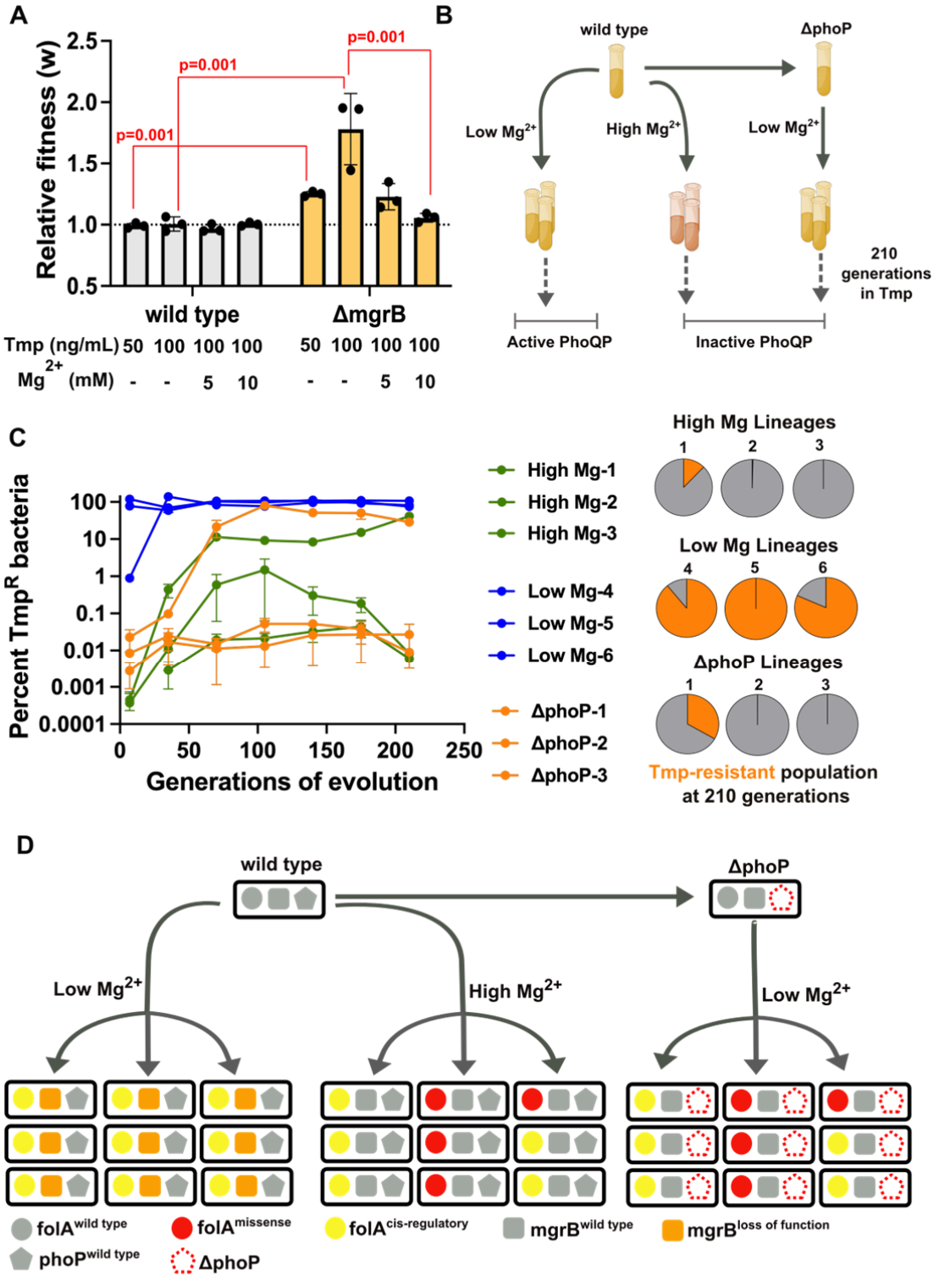

705
706

707 **Figure 2. Loss of MgrB facilitates the evolution of trimethoprim resistance in *E. coli*. A.**
708 Relative fitness (w) of *E. coli* wild type (gray) and an *mgrB*-knockout (orange) strain
709 compared to an isogenic *lacZ*-knock out reference strain. Relative fitness was calculated in
710 different concentrations of trimethoprim (Tmp) and $MgSO_4$ as indicated. Individual replicates
711 are plotted as black circles, and the mean value is shown as a bar. Error bars represent
712 standard deviation. A value of 1 (dotted line) indicates no change in fitness compared to the
713 reference strain. Statistical significance was tested using a Student's t-test and p-values are
714 shown for relevant comparisons. **B.** Schematic for laboratory evolution to investigate the
715 contribution of *mgrB*-mutations to trimethoprim resistance. Triplicate lineages were evolved
716 for ~210 generations in media supplemented with sub-MIC trimethoprim (100 ng/mL) in the
717 presence or absence of 10 mM $MgSO_4$. An additional 3 lineages were also evolved starting
718 with an isogenic *ΔphoP* strain in the absence of $MgSO_4$. The status of PhoQP activity in each
719 of the conditions is indicated. **C.** Numbers of trimethoprim-resistant bacteria from evolving
720 populations shown in B. Left panel: Titers of resistant bacteria at different generations of
721 evolution under active and inactive PhoP conditions expressed as a percentage of total
722 population. Right panel: Resistant fraction for each of the 9 lineages at 210 generations of
723 evolution (orange) shown as pie charts. **D.** Diagrammatic summary of genome sequencing for
724 3 randomly picked trimethoprim-resistant isolates from each of the 9 lineages in B and C.
725 The *folA* gene is represented by a circle, *mgrB* by a square and *phoP* by a pentagon. Gray
726 filled symbols indicate wild type alleles, while coloured symbols indicate mutations as shown
727 in the key.
728

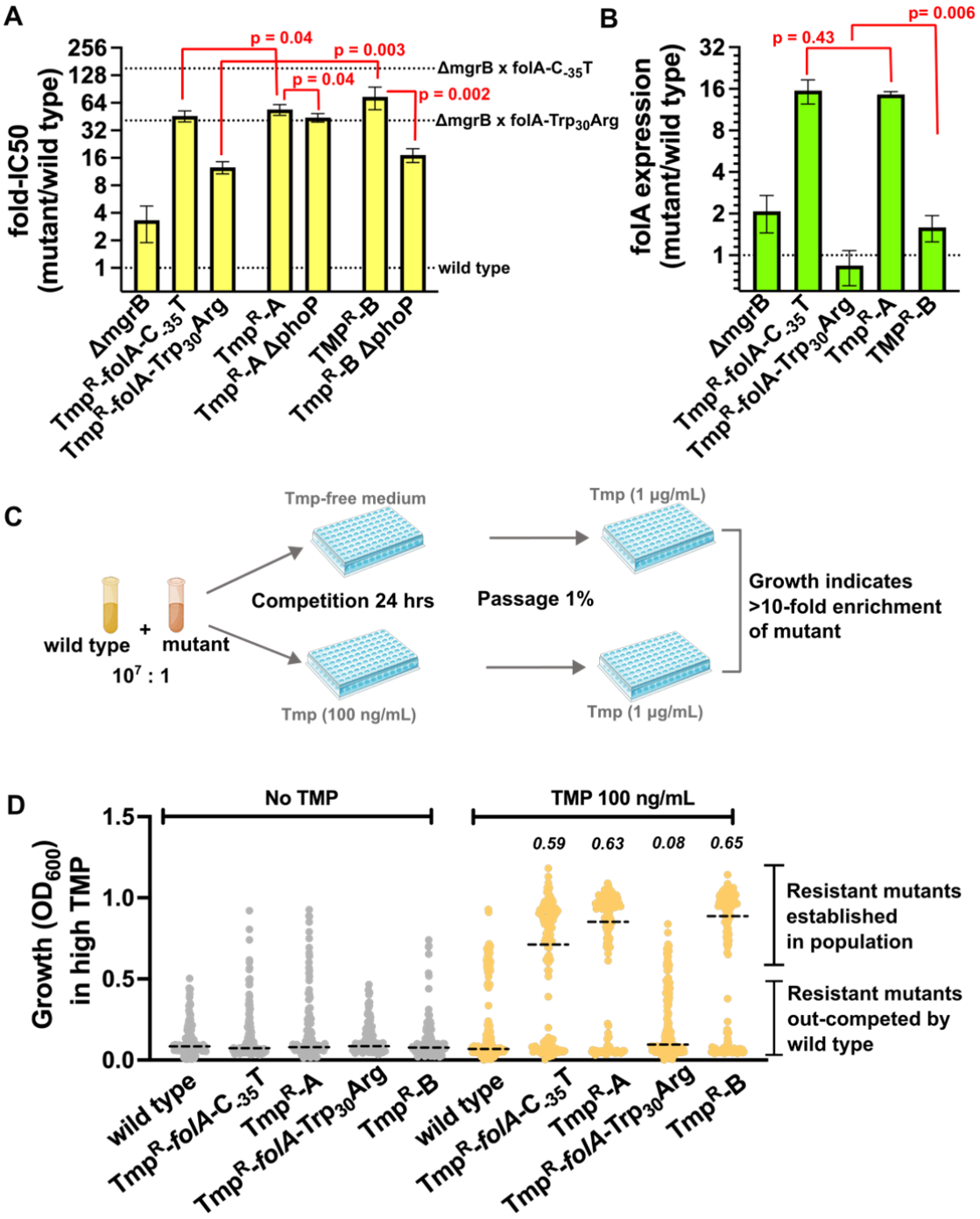

Figure 3. Epistasis between *mgrB* and *folA* mutations facilitate fixation of resistant bacteria. A. Fold change in trimethoprim IC_{50} values over wild type *E. coli* for indicated resistant strains are plotted as mean ± SD from 3 independent measurements. Statistical significance was tested using a Student's t-test and p-values for relevant comparisons are shown. Expected values for indicated combinations of mutations based on a non-epistatic/additive model are shown as dotted lines. **B.** Expression level of the *folA* gene measured by quantitative RT-PCR in trimethoprim resistant strains, normalized to wild type (=1; dotted line) are shown as bars. Mean ± SD from 3 independent experiments is plotted

739 and p-values from Student's t-test for relevant comparisons are shown. **C.** Experimental
740 design for estimating the establishment probability of resistant mutants over wild type. Mixed
741 strain cultures were set up with wild type in a large excess. Replicates (144 for each
742 comparison) were set up in 96-well plates in drug-free or trimethoprim-supplemented (100
743 ng/mL) media and allowed to grow for 24 hours. An aliquot (1%) of the culture was passaged
744 into media containing high trimethoprim (1 μg/mL i.e. MIC of wild type). Growth in high
745 trimethoprim would be observed only in those cases where the resistant mutant had been
746 enriched by >10-fold **D.** Scatter plot of OD values (at 600 nm) for all 144 competitions
747 carried out to determine establishment propensity. Monocultures of wild type and
748 competitions in drug-free media (gray) were used as controls to negate the effect of
749 spontaneous resistant mutants emerging during the assay. Competitions in trimethoprim-
750 supplemented media are plotted in ochre. Median OD values are shown as dashed lines. The
751 fraction of replicates in which the mutant was enriched compared to wild type based on
752 visible growth is indicated above the appropriate OD scatter.
753

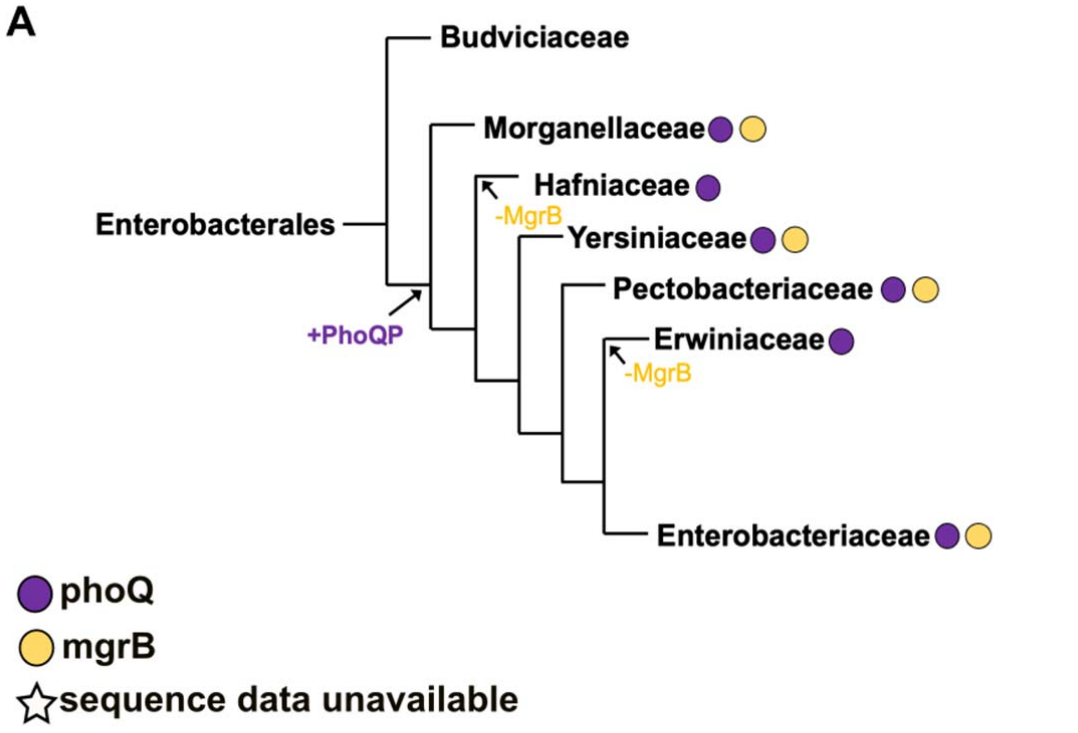
A
Budviciaceae
Morganellaceae
Hafniaceae
-MgrB
Enterobacterales
Yersiniaceae
Pectobacteriaceae
+PhoQP
Erwiniaceae
-MgrB
Enterobacteriaceae
phoQ
mgrB
sequence data unavailable

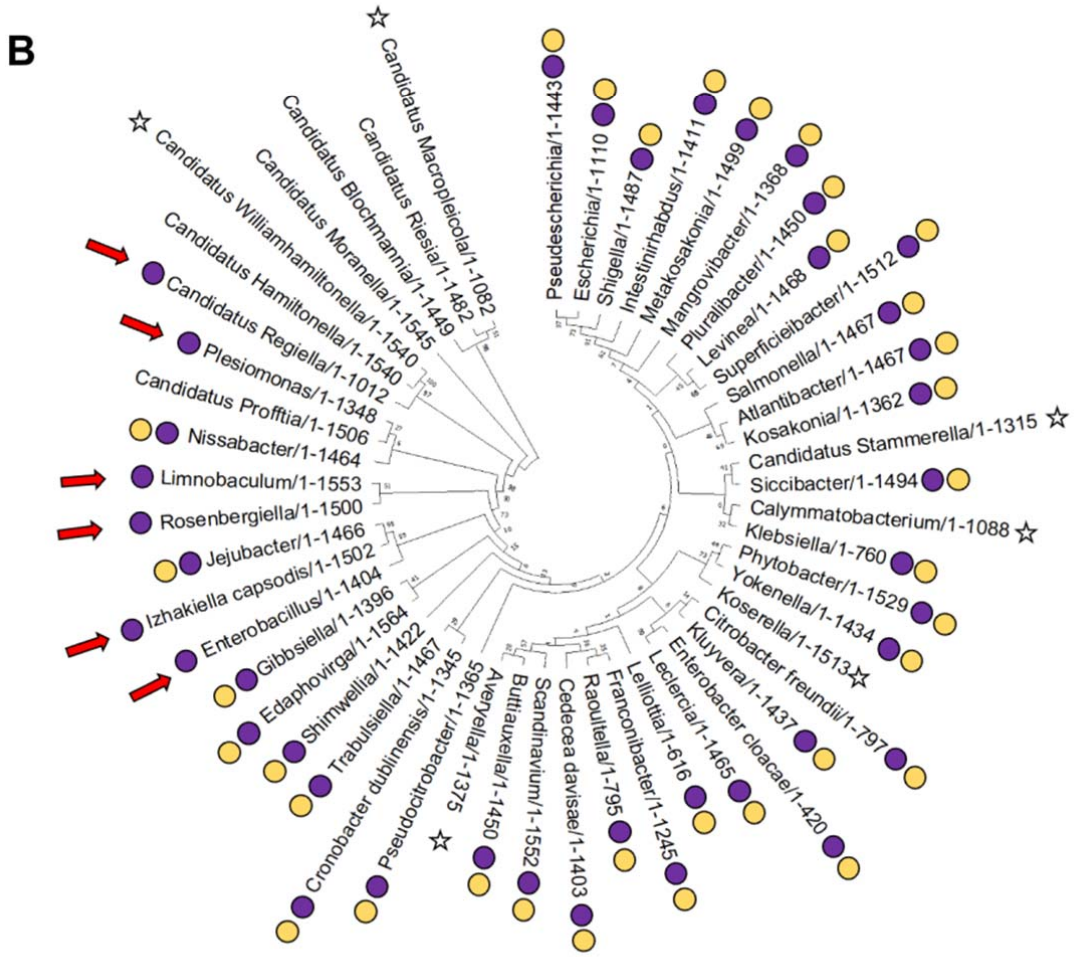
B
Candidatus Macropleicola/1-1082
Candidatus Riesia/1-1482
Candidatus Blochmannia/1-1449
Candidatus Moranella/1-1545
Candidatus Williamhamiltonella/1-1540
Candidatus Hamiltonella/1-1540
Candidatus Regiella/1-1012
Plesiomonas/1-1348
Candidatus Profftia/1-1506
Nissabacter/1-1464
Limnobaculum/1-1553
Rosenbergiella/1-1500
Jejubacter/1-1466
Izhakiella capsodis/1-1502
Enterobacillus/1-1404
Gibbsiella/1-1396
Edaphovirga/1-1564
Shimwellia/1-1422
Trabulsiella/1-1467
Cronobacter dublinensis/1-1345
Pseudocitrobacter/1-1365
Avenyella/1-1375
Buttiauxella/1-1450
Scandinavium/1-1552
Cedecea davisae/1-1403
Raoultella/1-795
Francoibacter/1-1245
Leliottia/1-616
Leclercia/1-1465
Enterobacter cloacae/1-420
Kluyvera/1-1437
Citrobacter freundii/1-797
Koserella/1-1513
Yokenella/1-1434
Phytobacter/1-1529
Klebsiella/1-760
Calymmatobacterium/1-1088
Siccibacter/1-1494
Candidatus Stammerella/1-1315
Kosakonia/1-1362
Atlantibacter/1-1467
Salmonella/1-1467
Superficieibacter/1-1512
Levinea/1-1468
Pluralibacter/1-1450
Mangrovibacter/1-1368
Metakosakonia/1-1499
Intestinirhabdus/1-1411
Shigella/1-1487
Escherichia/1-1110
Pseudescherichia/1-1443

Figure 4. Phylogenetic distribution of *mgrB* and *phoQ* genes across bacteria. A. Representation of the phylogenetic relationships between 7 bacterial families that make up the Order Enterobacterales, taken from Adelou et al., 2016 [44]. The presence of *mgrB* and *phoQ* genes in representative members of these families are shown as yellow and purple circles respectively. Most probable events of gain of the PhoQP system and loss of MgrB are indicated. **B.** Maximum Likelihood phylogeny of 61 representative species belonging to Family Enterobacteriaceae constructed using 16S rRNA sequences is shown. The presence of *phoQ* and *mgrB* are indicated by purple and yellow circles next to each species. Lack of annotated genome data is indicated by a star. Possible events of *mgrB*-loss are shown as red arrows.

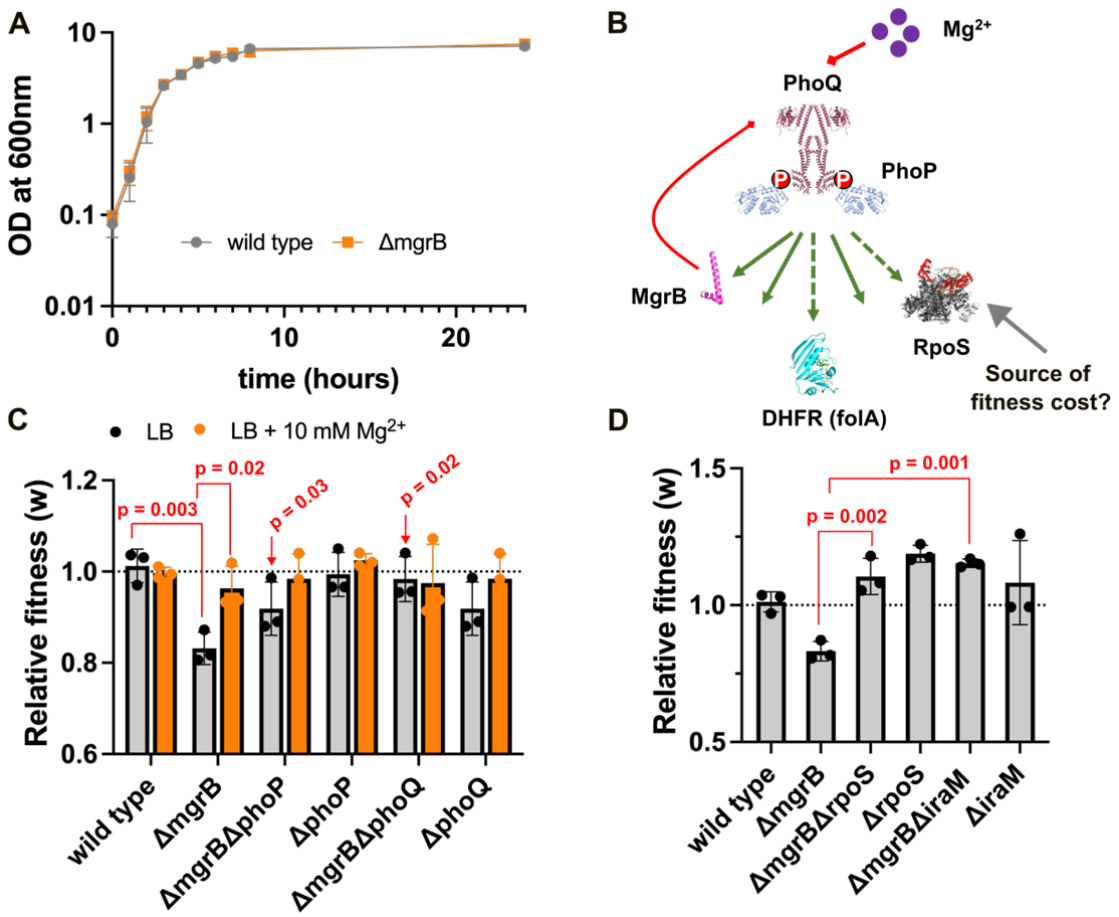

Figure 5. Loss of negative feedback is costly for *E. coli* due to PhoQP hyperactivity A. Growth curves of wild type *E. coli* and an isogenic *mgrB*-knockout strain *(ΔmgrB*) under standard growth conditions in LB. Growth was measured using OD at 600 nm. Mean ± SD from 3 independent experiments is plotted. **B.** Diagrammatic representation of the PhoQP signaling pathway (not to scale). Direct and indirect positive regulation by PhoP is shown as solid and dashed green arrows respectively. Inhibitory interactions are shown in red. AlphaFold models/crystal structures are used to represent proteins in the pathway that are relevant to this study. Source of the fitness cost of *mgrB*-deficiency based on our study is shown. **C and D.** Relative fitness (w) of *E. coli* wild type and indicated mutant strains compared to a *lacZ*-knock out reference strain calculated in LB (gray bars; low Mg^{2+}) or LB + 10 mM $MgSO_4$ (orange bars). Mean value from three independent experiments are plotted as bars, and individual values are shown. Error bars represent standard deviation. A value of 1 represents no change in fitness compared to the reference strain and is shown as a dotted line. Statistical significance was tested using a Student's t-test (p-values for relevant comparisons are shown). Double mutants were compared with *ΔmgrB* for statistically significant differences.

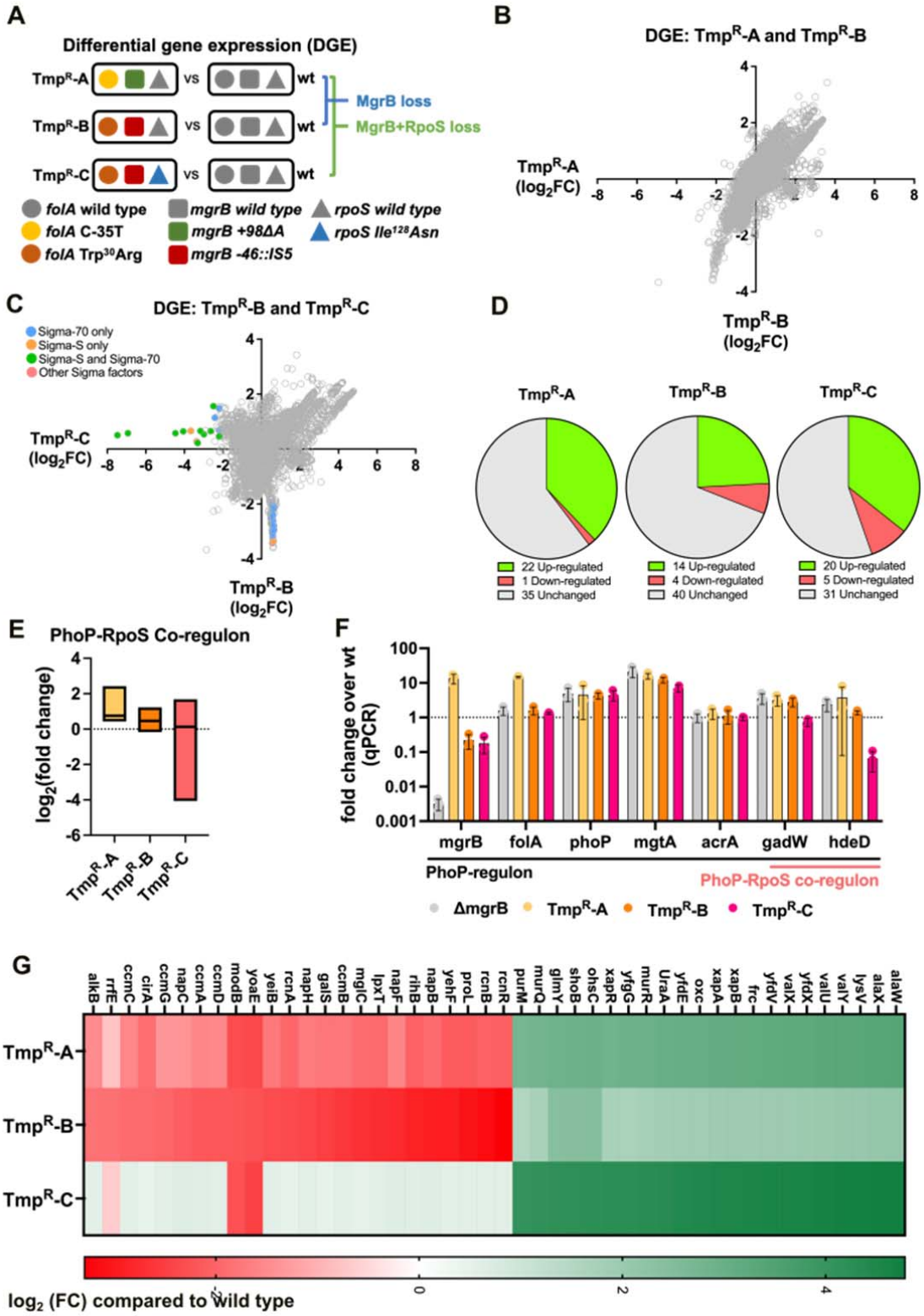

Figure 6. Transcriptional changes in trimethoprim resistant isolates explain the compensatory role of *rpoS* mutations A. Diagrammatic representation of the genotypes of strains used for RNA-sequencing based transcriptomics. Circles represent *folA*, squares

represent *mgrB* and triangles represent *rpoS*. Gray symbols represent wild type alleles, while coloured symbols represent mutant alleles as shown in the key. Comparisons between strains reveal the effects of *mgrB* and *mgrB*+*rpoS* mutations on the global transcriptome of *E. coli* as shown. **B.** Comparison of differential gene expression (DGE) between trimethoprim resistant strains Tmp^R-A and Tmp^R-B. For each strain DGE was estimated as log_2 of fold change compared to wild type (log_2FC). Each point on the scatter plot represents expression level of a single gene. **C.** Comparison of differential gene expression (DGE) between trimethoprim resistant strains Tmp^R-B and Tmp^R-C. For each strain DGE was estimated as log_2 of fold change compared to wild type (log_2FC). Each point on the scatter plot represents expression level of a single gene. For genes showing greater than 4-fold down-regulation in Tmp^R-B or Tmp^R-C compared to wild type, data points are colored by the sigma factor responsible for transcription as indicated based on data available on Ecocyc database [46]. **D.** Expression level of 58 genes of the PhoP regulon (gene list obtained from RegulonDB [47, 48]) in Tmp^R-A, B and C strains represented as pie-charts. Genes with at least 2-fold higher or lower expression level compared to wild type were classified as "up-regulated" or "down-regulated" respectively. **E.** Expression level of 14 genes co-regulated by PhoP and RpoS in Tmp^R-A, B and C strains shown as a box plot (min to max). The median expression level is shown by the line. **F.** Validation of RNA-sequencing based transcriptomics using quantitative RT-PCR (qPCR) for selected genes. Mean ± SD of fold change compared to the wild type from three independent biological replicates are plotted. No change in expression level compared to wild type corresponds to a value of '1' and is shown by a dotted line. Gene names are indicated on the X-axis. Different colours represent different strains from which measurements were made as shown in the key below the graph. **G.** Heat map showing expression level of RpoD-target genes in Tmp^R-A, B and C strains based on RNA-seq. For each strain, expression levels were compared to wild type and log_2(FC) is represented on a continuous red-green colour scale as shown.

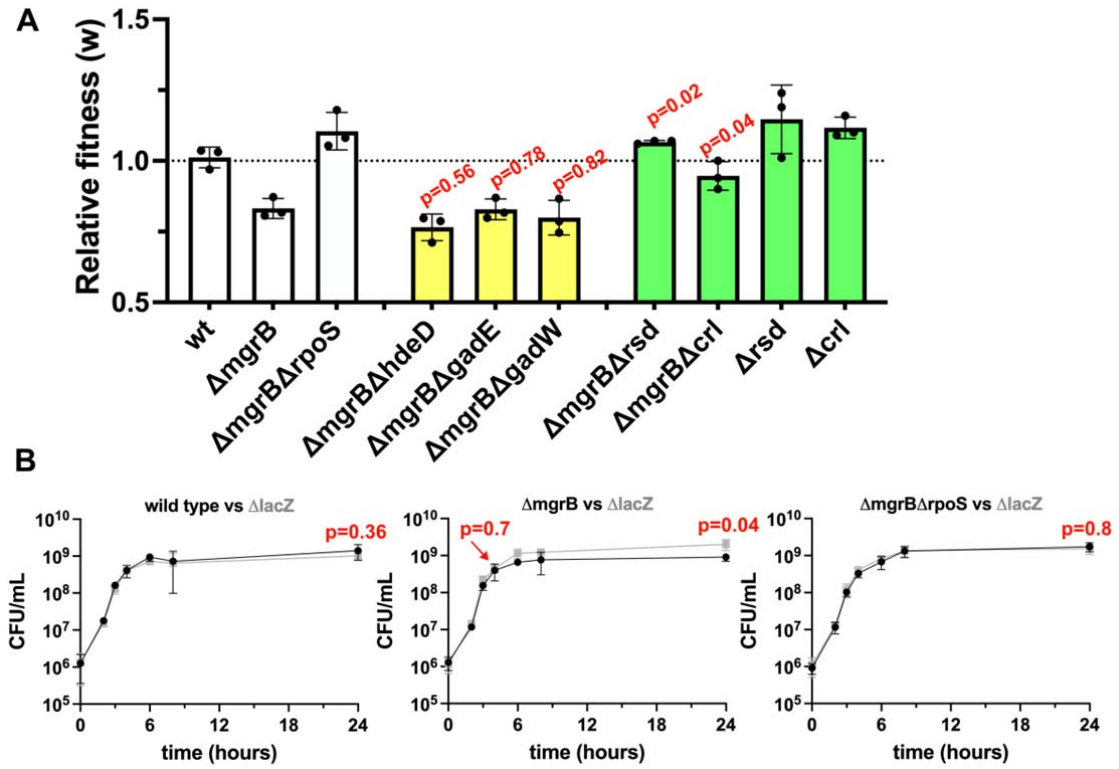

Figure 7. Loss of RpoS-RpoD balance explains the fitness costs of *mgrB*-deficiency A. Relative fitness (w) of *E. coli* wild type and indicated gene knockout strains compared to an isogenic *lacZ*-knock out reference strain in antibiotic-free media. Mean value from three independent experiments are plotted as bars. Error bars represent standard deviation. A value of '1' indicates no change in fitness compared to the reference strain and is shown as a dotted line. Yellow bars represent strains that were used to test the contribution of RpoS-targets to the costs of *mgrB*-deficiency, while green bars represent strains that were used to test the contribution of RpoS-RpoD imbalance to the costs of *mgrB*-deficiency. Statistical significance between the relative fitness of double mutants and *ΔmgrB* was tested using a Student's t-test (p-values shown above relevant bars). **B.** Growth of wild type, Δ*mgrB* or Δ*mgrB*Δ*rpoS* (black) in competition with an isogenic Δ*lacZ* strain (gray) over time expressed as CFUs/mL. Mean ± SD from three independent biological replicates is plotted. Student's t-test was used to compare statistical significance of the differences in bacterial densities of the competing strains (p-values are shown next to relevant data points).

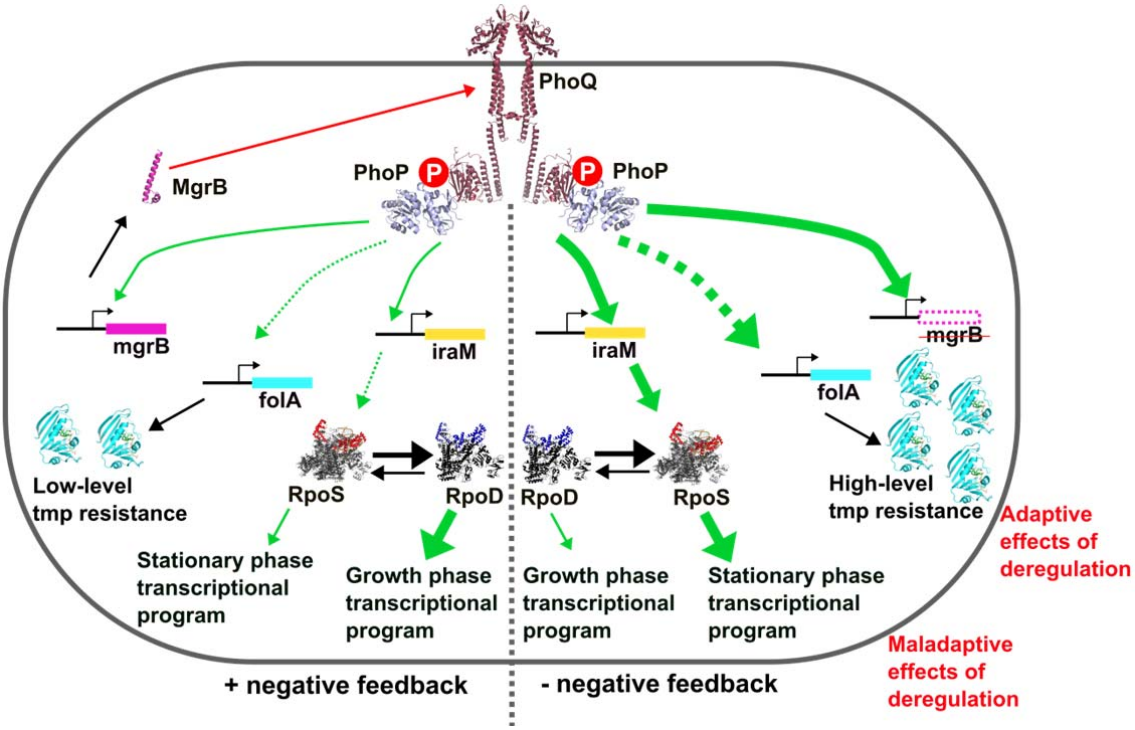

Figure 8. A gene regulatory model for the adaptive and maladaptive effects of deregulation in the PhoQP pathway. Diagrammatic representation of the proposed model for why deregulation of PhoQP due to loss of negative feedback regulator MgrB produces both adaptive and maladaptive gene regulatory changes. Left and right sides of the figure represent scenarios where negative feedback is retained or lost by the PhoQP system respectively. Direct and indirect effects are represented by solid and discontinuous arrows respectively. Positive regulation is represented by green arrows while negative regulation is represented by red arrows. Arrow thickness indicates strength of effect. Genes and their promoters are represented by boxes, while proteins are shown as structural models (Alphafold; https://alphafold.ebi.ac.uk/). The figure is not drawn to scale.

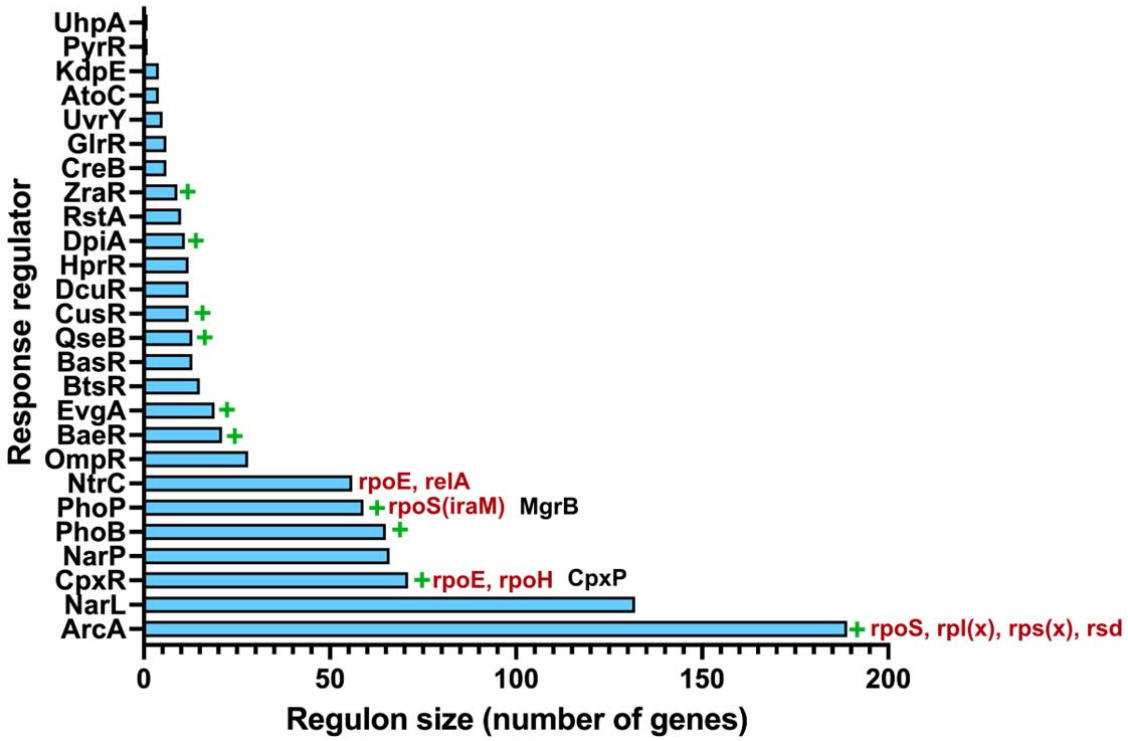

Figure 9. Regulon size and feedback in two-component systems of *E. coli*. Response regulators of 26 two-component systems from *E. coli* K-12 MG1655 ranked by their regulon sizes. Green plus sign (+) indicates that the two-component system is known to have positive feedback, i.e. stimulate its own transcription. Global regulators that these systems are known to cross-activate are in crimson next to respective response regulators, while known negative feedback regulatory proteins are in black. All information collated from Ecocyc [46].

858 **References**
859

860 1. Patel, V. and N. Matange, *Adaptation and compensation in a bacterial gene*
861 *regulatory network evolving under antibiotic selection.* Elife, 2021. **10**.
862 2. Ahnert, S.E. and T.M. Fink, *Form and function in gene regulatory networks: the*
863 *structure of network motifs determines fundamental properties of their dynamical*
864 *state space.* J R Soc Interface, 2016. **13**(120).
865 3. Dumont, J.E., et al., *Cross signaling, cell specificity, and physiology.* Am J Physiol
866 Cell Physiol, 2002. **283**(1): p. C2-28.
867 4. Becskei, A. and L. Serrano, *Engineering stability in gene networks by autoregulation.*
868 Nature, 2000. **405**(6786): p. 590-3.
869 5. Freeman, M., *Feedback control of intercellular signalling in development.* Nature,
870 2000. **408**(6810): p. 313-9.
871 6. Ji, N., et al., *Feedback control of gene expression variability in the Caenorhabditis*
872 *elegans Wnt pathway.* Cell, 2013. **155**(4): p. 869-80.
873 7. Kholodenko, B.N., *Cell-signalling dynamics in time and space.* Nat Rev Mol Cell
874 Biol, 2006. **7**(3): p. 165-76.
875 8. Smits, W.K., O.P. Kuipers, and J.W. Veening, *Phenotypic variation in bacteria: the*
876 *role of feedback regulation.* Nat Rev Microbiol, 2006. **4**(4): p. 259-71.
877 9. Shudo, E., P. Haccou, and Y. Iwasa, *Optimal choice between feedforward and*
878 *feedback control in gene expression to cope with unpredictable danger.* J Theor Biol,
879 2003. **223**(2): p. 149-60.
880 10. Dubnau, D. and R. Losick, *Bistability in bacteria.* Mol Microbiol, 2006. **61**(3): p.
881 564-72.
882 11. Hooshangi, S. and R. Weiss, *The effect of negative feedback on noise propagation in*
883 *transcriptional gene networks.* Chaos, 2006. **16**(2): p. 026108.
884 12. Zhang, H., Y. Chen, and Y. Chen, *Noise propagation in gene regulation networks*
885 *involving interlinked positive and negative feedback loops.* PLoS One, 2012. **7**(12): p.
886 e51840.
887 13. Nevozhay, D., et al., *Negative autoregulation linearizes the dose-response and*
888 *suppresses the heterogeneity of gene expression.* Proc Natl Acad Sci U S A, 2009.
889 **106**(13): p. 5123-8.
890 14. Hoch, J.A., *Two-component and phosphorelay signal transduction.* Curr Opin
891 Microbiol, 2000. **3**(2): p. 165-70.
892 15. Koretke, K.K., et al., *Evolution of two-component signal transduction.* Mol Biol Evol,
893 2000. **17**(12): p. 1956-70.
894 16. Stock, A.M., V.L. Robinson, and P.N. Goudreau, *Two-component signal*
895 *transduction.* Annu Rev Biochem, 2000. **69**: p. 183-215.
896 17. Kenney, L.J., *How important is the phosphatase activity of sensor kinases?* Curr Opin
897 Microbiol, 2010. **13**(2): p. 168-76.
898 18. Wall, E., N. Majdalani, and S. Gottesman, *The Complex Rcs Regulatory Cascade.*
899 Annu Rev Microbiol, 2018. **72**: p. 111-139.
900 19. Agrawal, R., B.K. Sahoo, and D.K. Saini, *Cross-talk and specificity in two-component*
901 *signal transduction pathways.* Future Microbiol, 2016. **11**: p. 685-97.
902 20. Laub, M.T. and M. Goulian, *Specificity in two-component signal transduction*
903 *pathways.* Annu Rev Genet, 2007. **41**: p. 121-45.
904 21. Singh, K., D.B. Senadheera, and D.G. Cvitkovitch, *An intimate link: two-component*
905 *signal transduction systems and metal transport systems in bacteria.* Future
906 Microbiol, 2014. **9**(11): p. 1283-93.

907 22. Groisman, E.A., *The pleiotropic two-component regulatory system PhoP-PhoQ.* J
908 Bacteriol, 2001. **183**(6): p. 1835-42.
909 23. Peterson, C.N., M.J. Mandel, and T.J. Silhavy, *Escherichia coli starvation diets:*
910 *essential nutrients weigh in distinctly.* J Bacteriol, 2005. **187**(22): p. 7549-53.
911 24. Otto, M., *Bacterial sensing of antimicrobial peptides.* Contrib Microbiol, 2009. **16**: p.
912 136-149.
913 25. Kleerebezem, M., et al., *Quorum sensing by peptide pheromones and two-component*
914 *signal-transduction systems in Gram-positive bacteria.* Mol Microbiol, 1997. **24**(5):
915 p. 895-904.
916 26. Jordan, S., M.I. Hutchings, and T. Mascher, *Cell envelope stress response in Gram-*
917 *positive bacteria.* FEMS Microbiol Rev, 2008. **32**(1): p. 107-46.
918 27. MacRitchie, D.M., et al., *Two-component signaling and gram negative envelope*
919 *stress response systems.* Adv Exp Med Biol, 2008. **631**: p. 80-110.
920 28. Bem, A.E., et al., *Bacterial Histidine Kinases as Novel Antibacterial Drug Targets.*
921 ACS Chemical Biology, 2015. **10**(1): p. 213-224.
922 29. Gotoh, Y., et al., *Two-component signal transduction as potential drug targets in*
923 *pathogenic bacteria.* Curr Opin Microbiol, 2010. **13**(2): p. 232-9.
924 30. Stephenson, K. and J.A. Hoch, *Two-component and phosphorelay signal-transduction*
925 *systems as therapeutic targets.* Curr Opin Pharmacol, 2002. **2**(5): p. 507-12.
926 31. Roggiani, M., S.S. Yadavalli, and M. Goulian, *Natural variation of a sensor kinase*
927 *controlling a conserved stress response pathway in Escherichia coli.* PLoS Genet,
928 2017. **13**(11): p. e1007101.
929 32. Domenech, P., et al., *Unique Regulation of the DosR Regulon in the Beijing Lineage*
930 *of Mycobacterium tuberculosis.* J Bacteriol, 2017. **199**(2).
931 33. Fallow, A., P. Domenech, and M.B. Reed, *Strains of the East Asian (W/Beijing)*
932 *lineage of Mycobacterium tuberculosis are DosS/DosT-DosR two-component*
933 *regulatory system natural mutants.* J Bacteriol, 2010. **192**(8): p. 2228-38.
934 34. Lippa, A.M. and M. Goulian, *Feedback inhibition in the PhoQ/PhoP signaling system*
935 *by a membrane peptide.* PLoS Genet, 2009. **5**(12): p. e1000788.
936 35. Yadavalli, S.S., et al., *Functional determinants of a small protein controlling a*
937 *broadly conserved bacterial sensor kinase.* J Bacteriol, 2020. **202**(16).
938 36. Rao, S.D. and O.A. Igoshin, *Overlaid positive and negative feedback loops shape*
939 *dynamical properties of PhoPQ two-component system.* PLoS Comput Biol, 2021.
940 **17**(1): p. e1008130.
941 37. Salazar, M.E., A.I. Podgornaia, and M.T. Laub, *The small membrane protein MgrB*
942 *regulates PhoQ bifunctionality to control PhoP target gene expression dynamics.* Mol
943 Microbiol, 2016. **102**(3): p. 430-445.
944 38. Shi, H., et al., *MgrB Inactivation Confers Trimethoprim Resistance in Escherichia*
945 *coli.* Front Microbiol, 2021. **12**: p. 682205.
946 39. Poirel, L., et al., *The mgrB gene as a key target for acquired resistance to colistin in*
947 *Klebsiella pneumoniae.* Journal of Antimicrobial Chemotherapy, 2014. **70**(1): p. 75-
948 80.
949 40. Zong, Z., Y. Feng, and A. McNally, *Carbapenem and Colistin Resistance in*
950 *Enterobacter: Determinants and Clones.* Trends Microbiol, 2021. **29**(6): p. 473-476.
951 41. Minagawa, S., et al., *Identification and molecular characterization of the Mg2+*
952 *stimulon of Escherichia coli.* J Bacteriol, 2003. **185**(13): p. 3696-702.
953 42. Wistrand-Yuen, E., et al., *Evolution of high-level resistance during low-level*
954 *antibiotic exposure.* Nat Commun, 2018. **9**(1): p. 1599.
955 43. Mistry, J., et al., *Pfam: The protein families database in 2021.* Nucleic Acids Res,
956 2021. **49**(D1): p. D412-D419.

957 44. Adeolu, M., et al., *Genome-based phylogeny and taxonomy of the 'Enterobacteriales':*
958 *proposal for Enterobacterales ord. nov. divided into the families Enterobacteriaceae,*
959 *Erwiniaceae fam. nov., Pectobacteriaceae fam. nov., Yersiniaceae fam. nov.,*
960 *Hafniaceae fam. nov., Morganellaceae fam. nov., and Budviciaceae fam. nov.* Int J
961 Syst Evol Microbiol, 2016. **66**(12): p. 5575-5599.
962 45. Xu, J., et al., *MgrB affects the acid stress response of Escherichia coli by modulating*
963 *the expression of iraM.* FEMS microbiology letters, 2019. **366**(11): p. fnz123.
964 46. Keseler, I.M., et al., *The EcoCyc Database in 2021.* Front Microbiol, 2021. **12**: p.
965 711077.
966 47. Santos-Zavaleta, A., et al., *RegulonDB v 10.5: tackling challenges to unify classic and*
967 *high throughput knowledge of gene regulation in E. coli K-12.* Nucleic Acids Res,
968 2019. **47**(D1): p. D212-D220.
969 48. Santos-Zavaleta, A., et al., *A unified resource for transcriptional regulation in*
970 *Escherichia coli K-12 incorporating high-throughput-generated binding data into*
971 *RegulonDB version 10.0.* BMC Biol, 2018. **16**(1): p. 91.
972 49. Nystrom, T., *Growth versus maintenance: a trade-off dictated by RNA polymerase*
973 *availability and sigma factor competition?* Mol Microbiol, 2004. **54**(4): p. 855-62.
974 50. Jishage, M. and A. Ishihama, *A stationary phase protein in Escherichia coli with*
975 *binding activity to the major sigma subunit of RNA polymerase.* Proc Natl Acad Sci U
976 S A, 1998. **95**(9): p. 4953-8.
977 51. Piper, S.E., et al., *A global view of Escherichia coli Rsd protein and its interactions.*
978 Mol Biosyst, 2009. **5**(12): p. 1943-7.
979 52. Pratt, L.A. and T.J. Silhavy, *Crl stimulates RpoS activity during stationary phase.*
980 Mol Microbiol, 1998. **29**(5): p. 1225-36.
981 53. Satishkumar, N., et al., *PBP4-mediated β-lactam resistance among clinical strains of*
982 *Staphylococcus aureus.* Journal of Antimicrobial Chemotherapy, 2021. **76**(9): p.
983 2268-2272.
984 54. Wright, M.S., et al., *Genomic and transcriptomic analyses of colistin-resistant*
985 *clinical isolates of Klebsiella pneumoniae reveal multiple pathways of resistance.*
986 Antimicrob Agents Chemother, 2015. **59**(1): p. 536-43.
987 55. Vilcheze, C. and W.R. Jacobs, Jr., *Resistance to Isoniazid and Ethionamide in*
988 *Mycobacterium tuberculosis: Genes, Mutations, and Causalities.* Microbiol Spectr,
989 2014. **2**(4): p. MGM2-0014-2013.
990 56. Matange, N., et al., *Trade-offs with stability modulate innate and mutationally*
991 *acquired drug resistance in bacterial dihydrofolate reductase enzymes.* Biochem J,
992 2018. **475**(12): p. 2107-2125.
993 57. Rodrigues, J.V., et al., *Biophysical principles predict fitness landscapes of drug*
994 *resistance.* Proc Natl Acad Sci U S A, 2016. **113**(11): p. E1470-8.
995 58. Maskell, J.P., A.M. Sefton, and L.M. Hall, *Multiple mutations modulate the function*
996 *of dihydrofolate reductase in trimethoprim-resistant Streptococcus pneumoniae.*
997 Antimicrob Agents Chemother, 2001. **45**(4): p. 1104-8.
998 59. Nyerges, A., et al., *Directed evolution of multiple genomic loci allows the prediction*
999 *of antibiotic resistance.* Proc Natl Acad Sci U S A, 2018. **115**(25): p. E5726-E5735.
1000 60. Toprak, E., et al., *Evolutionary paths to antibiotic resistance under dynamically*
1001 *sustained drug selection.* Nat Genet, 2011. **44**(1): p. 101-5.
1002 61. Matange, N., *Highly Contingent Phenotypes of Lon Protease Deficiency in*
1003 *Escherichia coli upon Antibiotic Challenge.* J Bacteriol, 2020. **202**(3).
1004 62. Händel, N., et al., *Interaction between mutations and regulation of gene expression*
1005 *during development of de novo antibiotic resistance.* Antimicrobial Agents and
1006 Chemotherapy, 2014. **58**(8): p. 4371-4379.

1007 63. Palmer, A.C., R. Chait, and R. Kishony, *Nonoptimal Gene Expression Creates Latent*
1008 *Potential for Antibiotic Resistance.* Mol Biol Evol, 2018. **35**(11): p. 2669-2684.
1009 64. Laws, M., A. Shaaban, and K.M. Rahman, *Antibiotic resistance breakers: current*
1010 *approaches and future directions.* FEMS Microbiol Rev, 2019. **43**(5): p. 490-516.
1011 65. Machado, D., et al., *Efflux Activity Differentially Modulates the Levels of Isoniazid*
1012 *and Rifampicin Resistance among Multidrug Resistant and Monoresistant*
1013 *Mycobacterium tuberculosis Strains.* Antibiotics, 2018. **7**(1): p. 18.
1014 66. Si, Z., et al., *Polymers as advanced antibacterial and antibiofilm agents for direct and*
1015 *combination therapies.* Chem Sci, 2022. **13**(2): p. 345-364.
1016 67. Dublanche, Y., et al., *Noise in transcription negative feedback loops: simulation and*
1017 *experimental analysis.* Mol Syst Biol, 2006. **2**: p. 41.
1018 68. Marciano, D.C., et al., *Negative feedback in genetic circuits confers evolutionary*
1019 *resilience and capacitance.* Cell Rep, 2014. **7**(6): p. 1789-95.
1020 69. Denby, C.M., et al., *Negative feedback confers mutational robustness in yeast*
1021 *transcription factor regulation.* Proc Natl Acad Sci U S A, 2012. **109**(10): p. 3874-8.
1022 70. Gogoleva, N., et al., *Transcriptomic dataset of wild type and phoP mutant*
1023 *Pectobacterium versatile.* Data Brief, 2020. **32**: p. 106123.
1024 71. Kravchenko, U., et al., *The PhoPQ Two-Component System Is the Major Regulator of*
1025 *Cell Surface Properties, Stress Responses and Plant-Derived Substrate Utilisation*
1026 *During Development of Pectobacterium versatile-Host Plant Pathosystems.* Frontiers
1027 in Microbiology, 2021. **11**.
1028 72. Perez, J.C., et al., *Evolution of a bacterial regulon controlling virulence and Mg(2+)*
1029 *homeostasis.* PLoS Genet, 2009. **5**(3): p. e1000428.
1030 73. Bray, A.S., et al., *MgrB-Dependent Colistin Resistance in Klebsiella pneumoniae Is*
1031 *Associated with an Increase in Host-to-Host Transmission.* mBio, 2022. **13**(2): p.
1032 e0359521.
1033 74. Groisman, E.A., *Feedback Control of Two-Component Regulatory Systems.* Annu
1034 Rev Microbiol, 2016. **70**: p. 103-24.
1035 75. Valverde, C. and D. Haas, *Small RNAs controlled by two-component systems.* Adv
1036 Exp Med Biol, 2008. **631**: p. 54-79.
1037 76. Vinchhi, R., C. Jena, and N. Matange, *Adaptive laboratory evolution of antimicrobial*
1038 *resistance in bacteria for genetic and phenotypic analyses.* STAR Protoc, 2023. **4**(1):
1039 p. 102005.
1040 77. Baba, T., et al., *Construction of Escherichia coli K-12 in-frame, single-gene knockout*
1041 *mutants: the Keio collection.* Mol Syst Biol, 2006. **2**: p. 2006 0008.
1042 78. Yamamoto, N., et al., *Update on the Keio collection of Escherichia coli single-gene*
1043 *deletion mutants.* Mol Syst Biol, 2009. **5**: p. 335.
1044 79. Parte, A.C., *LPSN--list of prokaryotic names with standing in nomenclature.* Nucleic
1045 Acids Res, 2014. **42**(Database issue): p. D613-6.
1046 80. Parte, A.C., et al., *List of Prokaryotic names with Standing in Nomenclature (LPSN)*
1047 *moves to the DSMZ.* Int J Syst Evol Microbiol, 2020. **70**(11): p. 5607-5612.
1048 81. Kumar, S., et al., *MEGA X: Molecular Evolutionary Genetics Analysis across*
1049 *Computing Platforms.* Mol Biol Evol, 2018. **35**(6): p. 1547-1549.
1050